Elimination of PZT Thin Film Breakage Caused By Electric Current Arcing and Intrinsic Differential Strains During Poling

by

AbdulelahAlsaeed

B.S. Mechanical Engineering
King Fahd University of Petroleum & Minerals, 2004

Submitted to the Department of Mechanical Engineering
in partial fulfillment of the requirements for the degree of

MASTER OF ENGINEERING IN MANUFACTURING

at the

MASSACHUSETTS INSTITUTE OF TECHNOLOGY

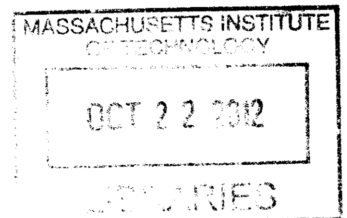

August 2012
[SEPTEMBER 2012]

© Massachusetts Institute of Technology, 2012. All rights reserved.

Author
Abdulelah I. Alsaeed
Department of Mechanical Engineering
10 August 2012

Certified by
Jung-Hoon Chun
Professor of Mechanical Engineering
Thesis Supervisor

Accepted by
David E. Hardt
Chairman, Departmental Committee on Graduate Studies
Department of Mechanical Engineering

Elimination of PZT Thin Film Breakage Caused By Electric Current Arcing and Intrinsic Differential Strains During Poling

by

Abdulelah Alsaeed

Submitted to the Department of Mechanical Engineering on 10 August, 2012,
in partial fulfillment of the requirements for the
Degree of Masters of Engineering in Manufacturing
Advisor: Prof. Jung-Hoon Chun

ABSTRACT

Historically, substrate breakage during the poling process has been responsible for a 2% yield loss for a contract manufacturer specializing in volume production of lead zirconate titatate (PZT) thin film devices. In this research, two major causes of poling breakage were identified. First, stresses along substrate edges make PZT substrates more susceptible to breakage if any sort of mechanical force is present. It was determined that these stresses were caused by differential strains due to incomplete metal layer coverage. Second, the electrical arcing that is frequently taking place during poling sends a mechanical shock wave through the substrate. Electrical arcing is caused by metal overspray during the sputtering process. Poling breakage was experimentally reduced by 70% by redesigning the shadow mask used during sputtering to eliminate any metal overspray.

Acknowledgements

I wish to extend my gratitude and thanks to my thesis supervisor Professor Jung-Hoon Chun for his guidance throughout this project. The time and care invested by my thesis supervisor has been greatly appreciated.

My gratitude and thanks is extended to my project teammates: Neha Dave and Jun Bum Lee. Their hard work, dedication and wonderful contributions helped carry out this project.

I owe my special thanks to the project host company management team for their hospitality and financial support. Special thanks go also to the PZT division employees for their understanding, excellent feedback and participation. Special thanks to project advisors: Eric and Mike.

Many thanks go to my academic advisor Professor David E. Hardt and to the Master of Engineering in Manufacturing program director Dr. Brian Anthony.

I am also grateful to a number of other people for their advice and input over the years, helping me to develop my experimental and analytical skills. In this regard, I would like to specifically thank Professor Hassan Badr, Professor Mohamed Habib, Associate Professor Esmail Mokheimer, Mr. Abbas Al-Maateeq, and Mr. Ahmed Al-Abbad.

Also, special thanks go to my wife Fatimah Al-Meer, for the love, unconditional support and friendship throughout the years.

Lastly, many thanks go to my family and friends for their patience and the support throughout my time at MIT.

Contents

CHAPTER 1 9
Introduction 9
1.1 Motivation 9
1.2 Objectives 10
1.3 Task Division 11
1.4 Process Overview 11
1.5 Approach 16
1.6 Thesis Structure 16
CHAPTER 2 17
Literature Review 17
2.1 Introduction 17
2.2 Piezoelectric and Ferroelectric Materials 17
2.2.1 Piezoelectric Effect 18
2.2.2 Pyroelectric Effect 19
2.2.3 Ferroelectric Effect 20
2.3 Lead Zirconate Titanate Piezo-ceramics 21
2.3.1 Crystalline Structure and Phase Relations 21
2.3.2 Compositional Modifications 24
2.3.3 Material Design 25
2.3.4 Manufacturing Method of Bulk PZT 25
2.4 Poling Process 28
2.4.1 Polarization Induced Stresses 29
2.4.2 Ions Doping and Poling 30
2.4.3 Liquid Dielectric and Poling 31

2.5 Sputtering Process 32
CHAPTER 3 34
Preliminary Analysis 34
3.1 PZT Substrate Breakage and Arcing 34
3.2 Chemical Analysis 36
3.3 Inconsistency in Metal Coverage 38
3.4 Potential Failure Modes 39
3.4.1 Electrical Arcing Due to External Nickel Overspray 39
3.4.2 Intrinsic Differential Strains Build Up during Poling 40
CHAPTER 4 42
Experimental Procedures 42
4.1 Nickel Overspray 42
4.2 Custom Imaging Mask 44
CHAPTER 5 46
Experimental Results and Discussion 46
5.1 Nickel Overspray 46
5.1.1 Reverse Sputtering 48
5.1.2 Low Poling Voltage 49
5.2 Custom Imaging Mask 50
5.2.1 Custom Imaging Mask Follow Up Experiment 51
5.3 Upgraded Sputtering Shadow Mask Design 53
CHAPTER 6 55
Conclusions, Recommendations and Future Work 55
APPENDIX A 58
Design of Experiment for Optimal Shadow Mask Design 58
APPENDIX B 59
Revision of Existing Shadow Mask Design 59
REFERENCES 66

List of Figures

Figure 1-1: Primary defects in 2011 10

Figure 1-2: Sputtering process; a) process starts with a PZT rectangular substrate with 0.2 mm (0.008 in) thickness; b) Sputtering of titanium tungsten adhesion layer; c) sputtering of nickel layer 12

Figure 1-3: Poling Process: a) metal coated PZT substrate with initial capacitance around 0.270 nF; b) application of voltage during poling: final capacitance around 0.400 nF caused by polarization increase during poling 13

Figure 1-4: Outline of manufacturing process for PZT thin films 15

Figure 2-1: a) low-temperature quartz simplified crystal structure; b) null dipole moment; and c) state of dipole moment (**δ**) 19

Figure 2-2: Pyroelectric crystal lattice representation. Change of permanent dipole moment due to application of force, change of temperature or electric field 20

Figure 2-3: Perovskite ABO3 structure; lead occupies A position, zirconium or titanium occupies B 22

Figure 2-4: Phase diagram of PbZrO3-PbTiO3 solid solutions 23

Figure 2-5: Effect of Zr/Ti ratio of PZT on piezoelectric properties; electromechanical coupling coefficient and piezoelectric d constant 23

Figure 2-6: Pb(Zr0.5Ti0.5)O3 powder preparation process 26

Figure 2-7: Grain growth and diffusion during sintering 27

Figure 2-8: Effect of sintering time on grain growth a) 1 hour and b) 16 hours 27

Figure 2-9: Polarization of PZT 28

Figure 2-10: correlation between electric field E and polarization P 29

Figure 2-11: Correlation between electric field and strain 30

Figure 2-12: Effect of acceptor and donor doping on PZT 31

Figure 2-13: Ballistic and diffuse transportation trajectory during sputtering 33

Figure 3-1: Substrate breakage and arcing; (a) substrate broken at poling; (b) magnified picture of arcing normally seen at substrate edges in case of breakage 35
Figure 3-2: Arcing marks reaching PZT material: a) arcing marks before etching; b) arcing marks on PZT material after etching..36
Figure 3-3: Chemical analysis result a) region 1: root; b) region 2: reference material............... 37
Figure 3-4: Inconsistency of metal coverage; Ni overspray on pattern side................................ 38
Figure 3-5: Substrates position inside shadow mask 39
Figure 3-6: Nickel overspray during sputtering that might lead to arcing................................... 40
Figure 3-7: (a) dipole moments random reorientation before poling; (b) poling with complete metal coverage; dipole moments reorientation takes place for entire substrate; (c) poling with edges exposed generates stresses at plane A and B due to differential strains.. 41
Figure 4-1: Custom imaging mask.. 44
Figure 5-1: Reduction of distance between metal sides after sanding edges; (a) initial space between metal sides; (b) effect of removal of PZT material and the reduction in space between metal sides...47
Figure 5-2: Reverse sputtering experiment: pattern side is coated with metal using the deeper side of the shadow mask instead of the shallower side 49
Figure 5-3: Differential strains experiment; a) outer frame free of metal coverage; b) middle area free of metal.. 52
Figure 5-4: Trial shadow mask with even depth for both sides.. 53
Figure 5-5: Effect of new shadow mask on metal overspray: (a) Substrate coated using new shadow mask showing metal free outer frame; (b) substrate coated using old shadow mask showing full metal coverage for pattern side......................................54

List of Tables

Table 2-1: Typical PZT ceramic applications and their required material properties..............24

Table 2-2: Breakdown voltages for typical semiconductor industry dielectric fluid compared to air and vacuum 32

Table 4-1: Nickel overspray experiment – no dielectric fluid..43

Table 4-2: Custom imaging mask experiment – no dielectric fluid..................................45

Table 5-1: Nickel overspray experiment results...48

Table 5-2: Custom imaging mask experiment results...51

CHAPTER 1

Introduction

1.1 Motivation

Historical data in Figure 1-1 show that volume production of lead zirconate titatate (PZT) thin film devices results in 15% of the devices with defects. These devices are rejected for excess metal defects, holes or voids in the pattern, or cracks and breaks in the ceramic material. Each lost device results in wasted material, labor time, and cost.

PZT thin film devices act as small scale circuits, consisting of a small ceramic surface with its wiring 'printed' onto the surface in specific, predetermined pattern. As electrical current moves through these metal surfaces, any misplaced metal or contaminants found on the surface can reduce or block the flow of current through the circuit. Thus, high quality devices must not have any surface or material defects.

Figure 1-1 shows percentage yield loss caused by each defect type:

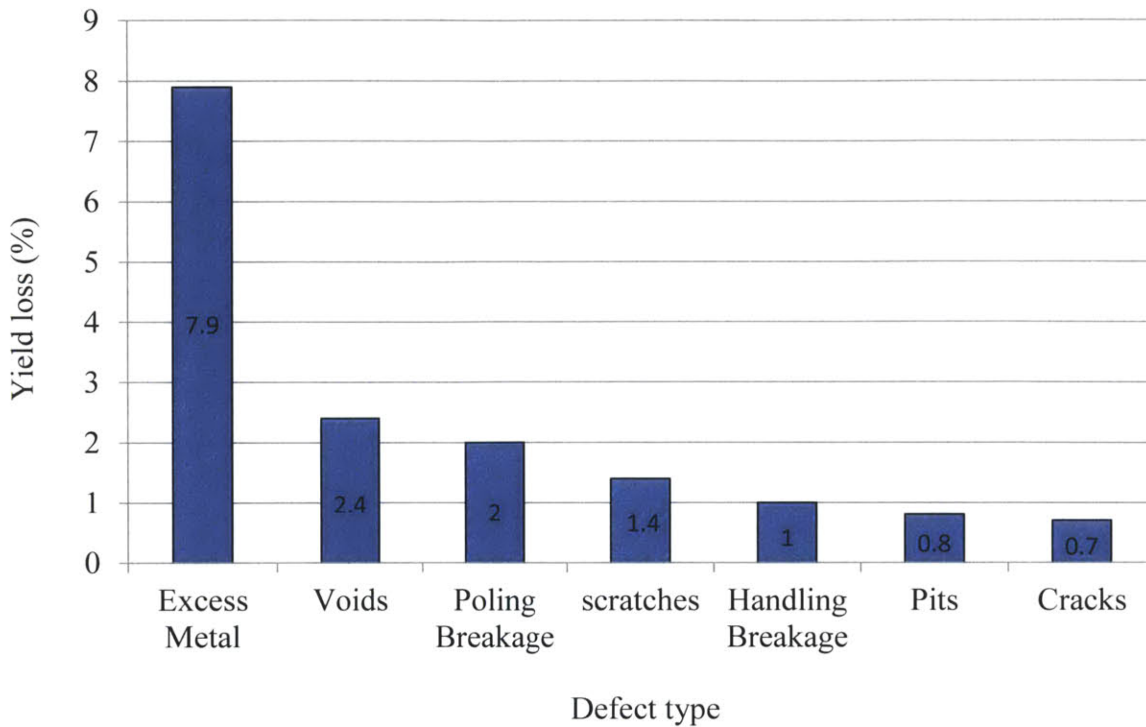

Figure 1-1: Primary defects in 2011.

1.2 Objectives

The principal objective of this project is to identify and eliminate the causes of defects with significant contribution to yield loss in order to increase the manufacturing yield. In order to achieve this improvement, the project was divided into three separate tasks, each established to target a leading cause of defective devices. These tasks are listed below:

- Eliminate excess metal defects and pattern voids due to defective photoresist coating
- Eliminate excess metal defects due to incomplete metal and oxide removal and
- Eliminate substrate breakage caused during the poling process

1.3 Task Division

The project was divided into the three tasks listed in Section 1.2. Each group member took the lead on one task. Jun Bum Lee [1] was responsible for the reduction of excess metal and void defects caused by defective photoresist quality, while Neha Dave [2] was responsible for the reduction of these defects as they related to etching. This author was responsible for the elimination of yield loss due to breakage inside the poling machine. All team members shared the underlying goal of yield improvement.

This thesis focuses on the poling breakage defect type. The following sections describe methods to identify the root cause of poling breakage and present recommendations to prevent its future occurrence.

1.4 Process Overview

The manufacturing process for PZT devices is initiated by coating the substrates, or ceramic wafers, with two metal layers. First, a single barrier layer of titanium tungsten (WTi) is deposited across the entire surface to promote its adhesion to the conductive metal layer. The WTi layer is 400 Angstroms in thickness. The coated substrate is then sputtered with a layer of nickel (Ni) which is intended to carry current through the device. The patterned substrate side is sputtered with 8000 Angstroms of Ni while the sacrificial side is only coated with a sacrificial layer of 1000 Angstroms of Ni. The 1000 Angstroms Ni layer represents an electrode that is needed for the poling process; the next step in the process. Figure 1-2 illustrates the sputtering process.

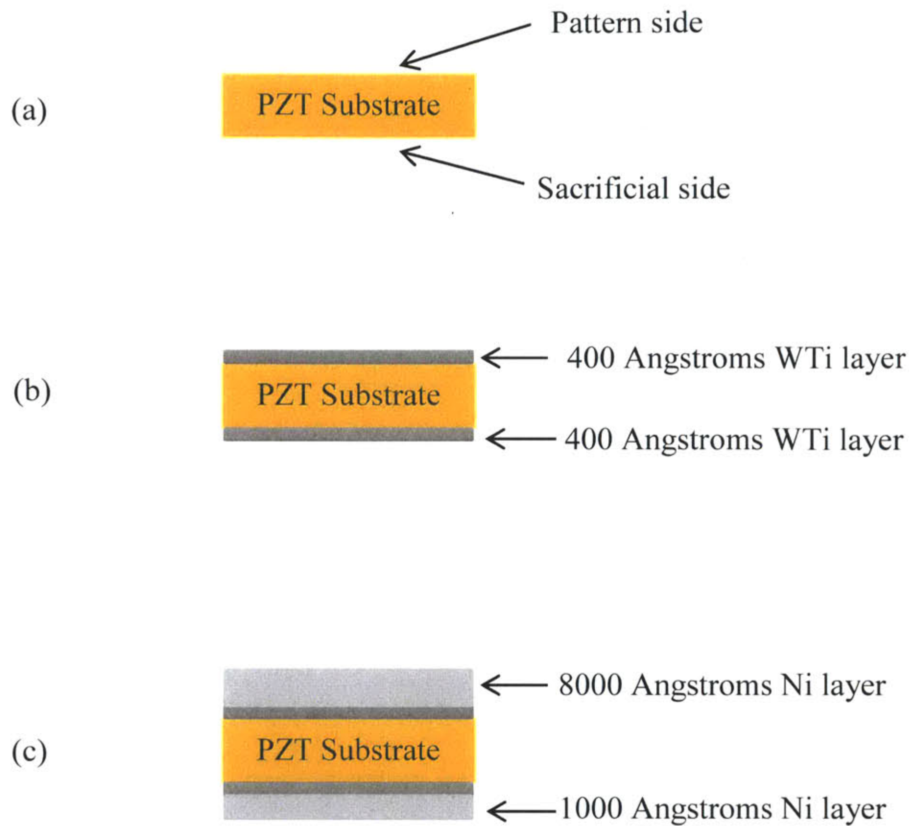

Figure 1-2: Sputtering process; a) process starts with a PZT rectangular substrate with 0.2 millimeters (0.008 in) thickness; b) Sputtering of titanium tungsten adhesion layer; c) sputtering of nickel layer.

During sputtering, a special fixture called a shadow mask is used to hold PZT substrates in place and to prevent substrate edges from being covered with metal to prevent any short circuit between the two metal sides.

The PZT substrate then undergoes a process called poling, which will change the PZT dipole moments molecular orientation to improve its piezoelectric properties. During poling, a custom designed machine is used. An electrical field of 1000 Volts is applied to increase polarization of PZT substrates. Polarization is measured in terms of final capacitance level. Typically, initial

capacitance value measured directly after sputtering is around 0.270 nanoFarads. At the poling process, at least a 32% increase in capacitance value is required. Typical final capacitance levels are in the range of 0.395 to 0.410 nanoFarads.

During the poling process, a dielectric fluid with a breakdown voltage of 35 kilovolts for 2.4 millimeters (0.1 inches) gap is used. The purpose of the dielectric fluid is to prevent any electrical current jump over between the two metal layers when the poling voltage is applied. For existing setup and parameters, used fluid provides a 2.8 kilovolts breakdown voltage assuming 0.2 millimeters (0.008 inches) wafer thickness and full substrate metal coverage. Throughout this thesis, mentioned electrical current jump over is referred to as poling arcing or simply arcing. Figure 1-3 presents the poling process.

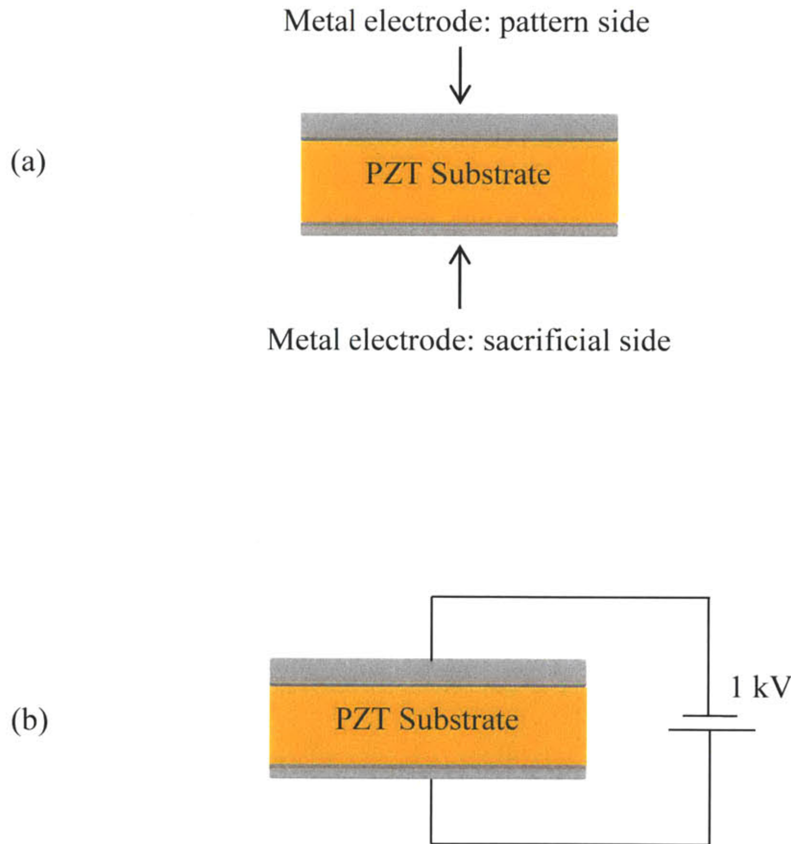

Figure 1-3: Poling Process: a) metal coated PZT substrate with initial capacitance around 0.270 nanoFarads; b) application of voltage during poling: final capacitance around 0.400 nanoFarards caused by polarization increase during poling.

During the voltage application in the poling process, substrates occasionally shatter inside the machine and must be scrapped. In 2011, 67% of the total yield loss due to PZT substrate breakage was in fact caused by breakage during poling which translates into 2% of total yield loss.

The patterning process then follows. First, the metalized substrates are sprayed with a protective photoresist layer. A mask with an image of the pattern is then placed on top of each substrate prior to exposing it to high intensity ultraviolet light. Any photoresist that was not shielded by the mask from the UV light will dissolve in the developing bath, leaving behind a pattern of intact photoresist in the shape of the circuit wiring. A wet etch process is then performed to remove metal in the non-patterned areas. The process of coating, imaging, and developing these substrates is collectively known as photolithography. At the end of the photolithography stage, the devices are electrically functional but still connected to each other on the substrate. To separate them, the substrates are diced into individual devices for final testing and application.

Throughout the manufacturing process, a number of visual and electrical quality inspections take place to quickly identify process control concerns. Rejected devices are typically eliminated in the final inspection stage in order to conserve the other devices on the substrate. Once the operators have verified the electrical and visual quality of all devices, they are carefully packaged and sent to the customer. Figure 1-4 outlines this high volume manufacturing process, as well as the basic function and primary source of yield loss at each stage.

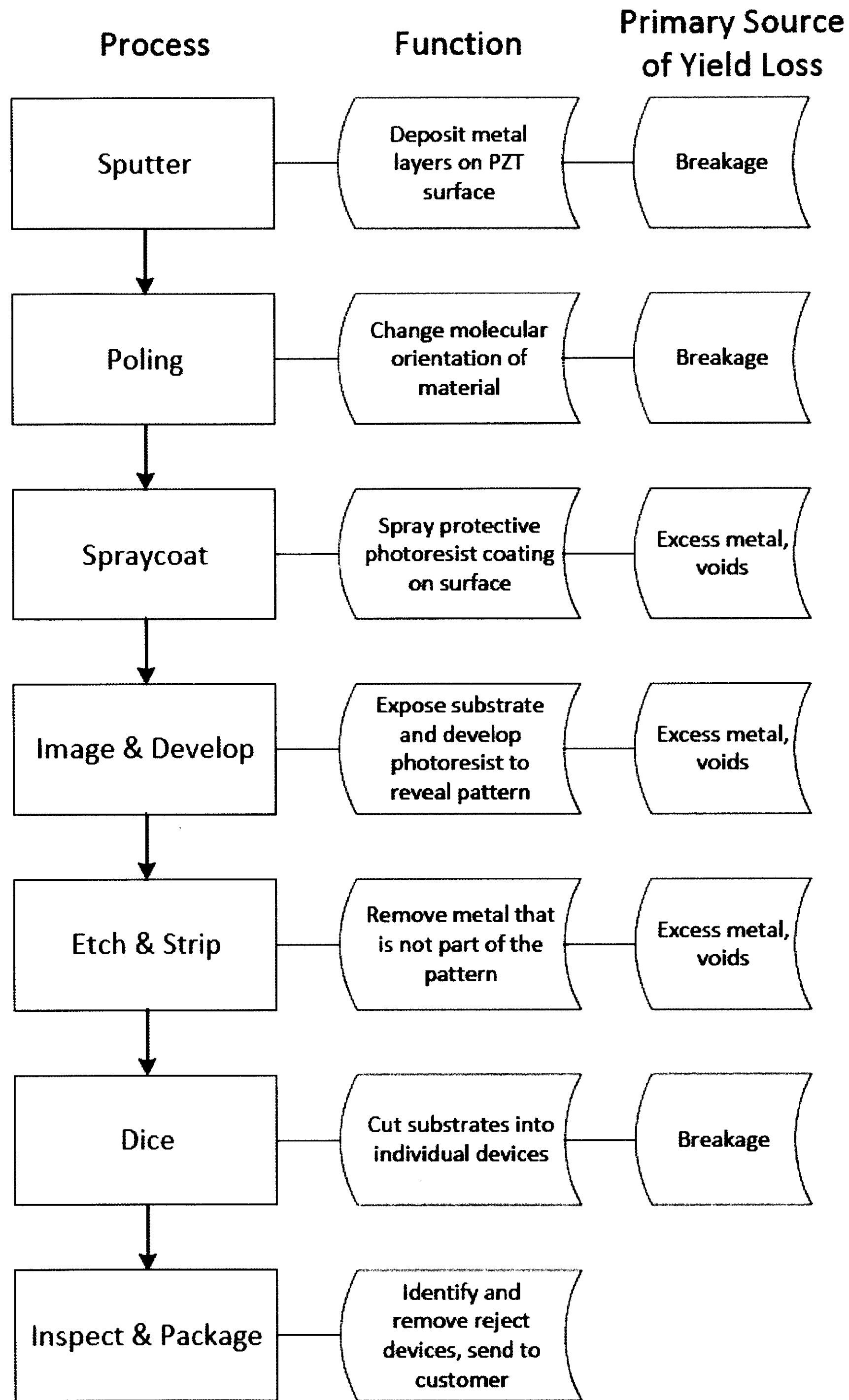

Figure 1-4: Outline of manufacturing process for PZT thin films.

1.5 Approach

Preliminary analysis of broken substrates in the poling process eliminated variables such as variation in thickness, breakage origin, chamber placement, operator error, and raw material defects as the cause of this phenomenon. Process observations, defect examination, and a detailed review of available literature were combined with experimentation to analyze the upstream metal deposition process and electrical properties of the piezoelectric material in order to eliminate this source of failure.

Outcomes of the preliminary analysis were combined with technical data obtained from literature to form a set of hypotheses to explain poling breakage phenomenon. These hypotheses were experimentally tested and validated. Once root cause behind the poling breakage was confirmed, efforts were switched to finding a way to eliminating it. A proposed remedy was then successfully tested.

1.6 Thesis Structure

This thesis is divided into 6 chapters. The introduction in Chapter 1 provides an outlook of the thesis in terms of motivation, objective, process overview, approach, and final findings. The literature review then follows in Chapter 2, where pertinent background information on piezoelectric and ferroelectric material, PZT, the poling process, and the sputtering process is included. In Chapter 3, a preliminary analysis of the poling breakage phenomenon is summarized. In this chapter, the two main causes behind the breakage during the poling process are presented. In Chapter 4, the experimental procedures that were followed to validate proposed causes are explained. In Chapter 5, the results of conducted experiments are discussed. This chapter also presents a suggested solution to the poling breakage problem that was successfully tested. Finally, conclusions, recommendations, and ideas for further work are presented in Chapter 6.

CHAPTER 2

Literature Review

2.1 Introduction

This thesis concludes that an intrinsic buildup of differential strains in PZT substrates during poling is a main cause of breakage during that process if a poling arcing is also present. It is also concluded that insufficient application of the metal layer during the sputtering step is ultimately causing both the differential strains and the frequent arcing during poling.

Thus, a thorough understanding of the piezoelectric behavior of PZT in general and during the poling process in particular is essential in order to explain the strain phenomenon. Also, a basic understanding of the metal sputtering process is also required to explain the inconsistency of metal layer coverage.

In this chapter, thesis pertinent background information is presented. To begin, an introductory description of piezoelectric and ferroelectric material is included. The focus is then narrows to provide background information specific to PZT. After that, there is a comprehensive discussion of the poling of process. Finally, several aspects of the sputtering process are highlighted.

2.2 Piezoelectric and Ferroelectric Materials

Crystal structures of materials are classified into 32 groups according to the number of rotational axes and reflection planes they display. The ability of these structures to show piezoelectric properties is determined based on the absence of structural symmetry, known as 'non-centrosymmetric.' The nonexistence of center of symmetry creates a dipole moment at the level of crystal lattice upon the application of a mechanical constraint by separating the center of

positive charges from that of the negative charges. This asymmetry is seen in 20 crystal structures out of the 32 classes and they are classified as piezoelectric [3].

2.2.1 Piezoelectric Effect

Piezoelectricity is the resultant electric charge accumulated by non-centrosymmetric structures upon application of mechanical strain. This phenomenon was discovered in 1880 by the Curie brothers. They discovered that single crystal quartz generate charge under pressure [4].

One year later, the piezoelectric effect was defined by Gabriel Lippmann as the 'linear electromechanical interaction of non-centrosymmetric crystalline materials.' Gabriel Lippmann recognized the geometrical strain of quartz when subjected to an electrical field. He noticed that piezoelectric effect is also reversible. Application of force generates an electrical charge and application of electrical field result in a mechanical strain. Also, reversing the force will lead to reversal of the dipole moment generated and increasing the force will lead to increasing the dipole moment magnitude [4].

Figure 2-1 illustrates this concept. Although dipole moments may exist in the neutral state, their summation is zero. This is shown in b. Yet, when force is applied in the vertical direction for example, as shown in c, a dipole moment is established in the horizontal direction [3]

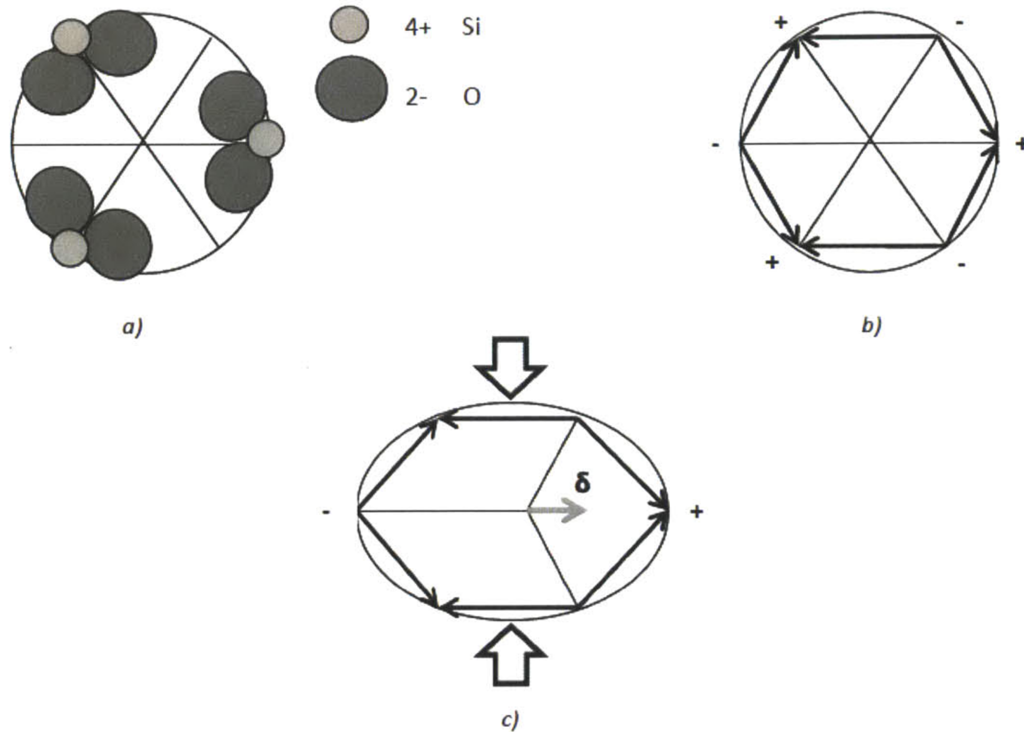

Figure 2- 1: a) low-temperature quartz simplified crystal structure; b) null dipole moment; and c) state of dipole moment (**δ**) [3].

2.2.2 Pyroelectric Effect

Ten of the 20 piezoelectric crystal structures, including that of PZT, are also characterized as pyroelectic. Pyroelectricity is the generation of temporary voltage that is caused by heating or cooling of material. Change in the temperature of the material causes a volumetric change. This change in volume changes the dipole length and subsequently the overall dipole moment charge intensity [3]. PZT is extremely sensitive to temperature variation as a result of its intrinsic pyroelectricity. Figure 2-2 illustrates the pyroelectric effect:

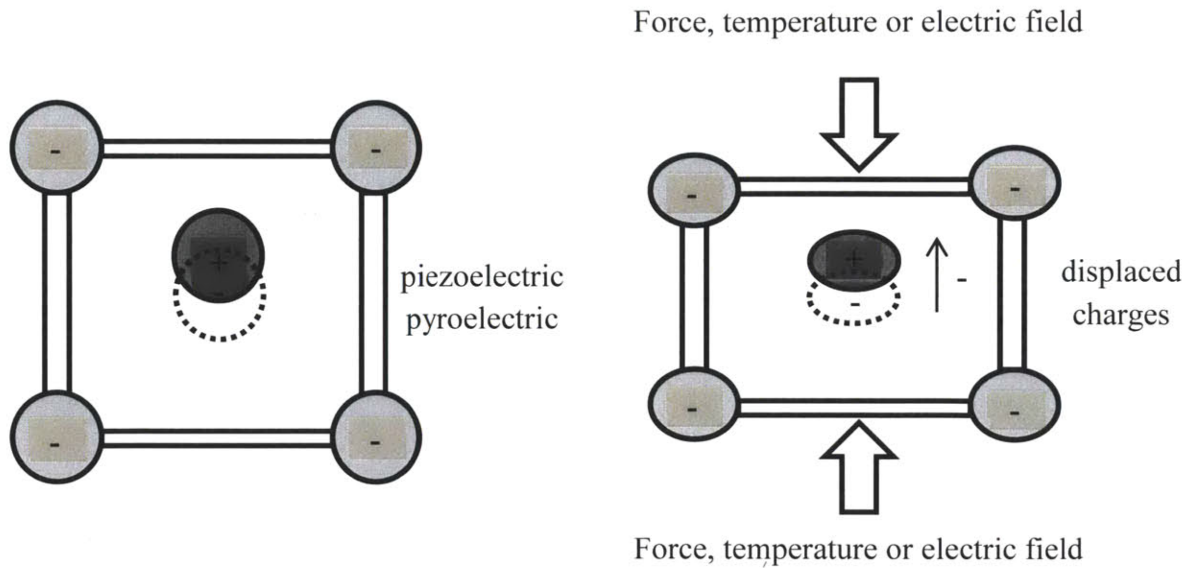

Figure 2- 2: Pyroelectric crystal lattice representation. Change of permanent dipole moment due to application of force, change of temperature or electric field [3].

2.2.3 Ferroelectric Effect

Among the 10 pyroelectric crystal structure classes of material with lattice structures having permanent dipole moments, there are some materials with spontaneous polarization that could be reversed if a high electrical field is applied, known as the ferroelectric effect. PZT is among this group [3].

The ferroelectric effect enables control of PZT strain behavior based on direction and magnitude of applied electrical field. That is why PZT thin films are used in a wide range of application.

2.3 Lead Zirconate Titanate Piezo-ceramics

PZT is a solid solution of lead zirconate, $PbZrO_3$, and lead titanate, $PbTiO_3$. It was first studied in 1952 by G. Shirane. Since then, it has been widely used in electronic applications due to its superior piezoelectric properties. PZT properties could be easily altered by different methods to satisfy different requirements. PZT based ceramics, like other ceramics, are also known for their good shaping flexibility. PZT based ceramics could be found in communication circuits, ultrasonic transducers, sensors and actuators applications [5].

2.3.1 Crystalline Structure and Phase Relations

As stated, PZT is a solid solution of $PbZrO_3$ and $PbTiO_3$. In practice, both components have a Perovskite-structure which is the final structure for sintered PZT. The perovskite crystalline structure promotes PZT's functionality as a good dielectric and piezoelectric material.

After mixing, $PbZrO_3$ and $PbTiO_3$ to form an ABO_3 structure [2]. As indicated in figure 2-3, lead atoms form a box around an octahedron of oxygen atoms. The oxygen octahedron contains either a zirconium or titanium atom as a center point. The dipole moment is formed between the zirconium or titanium ions as a center of the positive charge and the center of the oxygen octahedrons as the center of negative charge. As indicated in Section 2.2.3, for a ferroelectric material, this dipole moment could be increased or decreased in magnitude or even reversed in direction by the application of an electrical field [5].

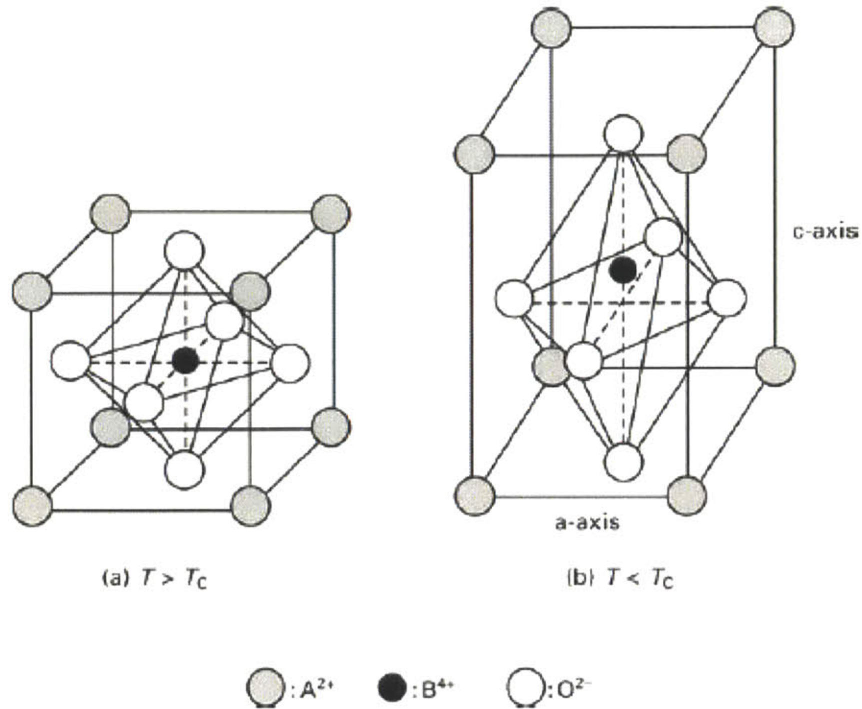

Figure 2- 3: Perovskite ABO3 structure; lead occupies A position, zirconium or titanium occupies B [5].

Based on the $PbZrO_3$ to $PbTiO_3$ composite ratio and temperature, PZT typically has a cubic, rhombohedral or tetragonal crystalline structure. Figure 2-4 shows the $PbZrO_3$-$PbTiO_3$ solid solutions phase diagram. The line that separates the rhombohedral and tetragonal phases is called the morphotropic phase boundary (MPB), and usually falls within the Zr/Ti ratio of 53 to 47 [5].

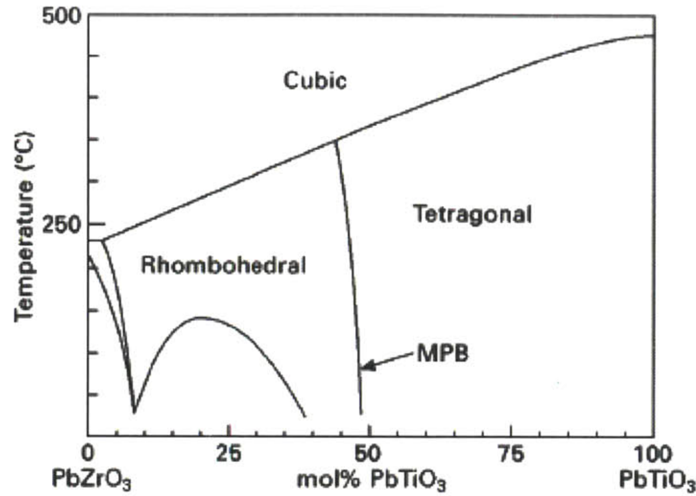

Figure 2- 4: Phase diagram of PbZrO3-PbTiO3 solid solutions [5].

It was observed that PZT ceramics with Zr/Ti ratio close to the MPB line have the highest electromechanically coupling coefficient and the highest piezoelectric constant which leads to the largest piezoelectric displacement [7]. Figure 2-5 illustrate this phenomenon.

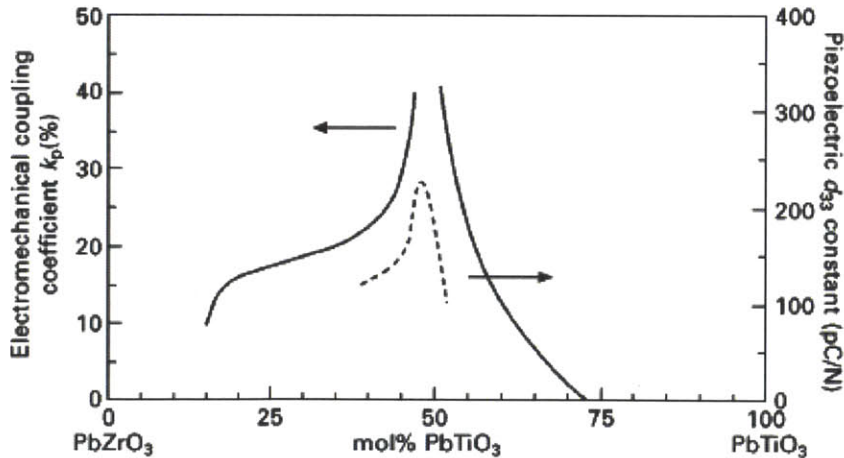

Figure 2- 5: Effect of Zr/Ti ratio of PZT on piezoelectric properties; electromechanical coupling coefficient and piezoelectric d constant [5].

2.3.2 Compositional Modifications

As indicated in Section 2.3.1, PZT composition or the Zr/Ti ratio has the biggest effect on final product properties. Changing the Zr/Ti ratio is in fact the main method that is utilized to adjust PZT properties in order to meet the different requirements for different applications in terms of temperature stability, piezoelectric constant, mechanical quality factor, or mechanical strength.

Another way to change final properties of PZT is the acceptor and donor ion doping. Here, ions are added to dilute Pb or Zr/Ti content. Common examples are adding potassium K^{1+} or iron Fe^{3+} ions to dilute Pb^{2+} or Zr^{4+}/Ti^{4+} effect, respectively. This is called acceptor doping. In this case, replacement ions have lower charge. In the case of donor doping, ions of higher charge are added such as Lanthanum La^{3+} or Niobium Nb^{5+} ions to replace Pb^{2+} or Zr^{4+}/Ti^{4+}, respectively. This process has a direct effect on material dipole moments and consequently on properties linked to PZT polarization.

An additional method by which PZT properties are enhanced or altered is by the addition of different perovskites crystalline materials that are known to improve final piezoelectric properties. A common example is $Pb(Sb_{1/2}Nb_{1/2})O_3$ that is used for communication circuits for its superior temperature stability [5].

Table 2-1 includes typical PZT ceramic applications and their required material properties.

Table 2- 1: Typical PZT ceramic applications and their required material properties [5]

Application	Required material characteristics
Inkjet actuator	Large d constant, low dielectric permittivity, high mechanical strength
Fuel injection actuator	Large d constant, high Curie temperature, high mechanical strength
Buzzer, loudspeaker	Large d constant, low dielectric constant, high mechanical strength
Shock sensor	Large d constant, large g constant
Ultrasonic motor	High Q_m, large coupling coefficient, high mechanical strength
Piezo gyroscope	High Q_m, large coupling coefficient, high mechanical strength
Resonator	Temperature stability, low aging, high Q_m
Filter	Temperature stability, low aging, large coupling coefficient

2.3.3 Material Design

As explained in Section 2.2.3, PZT is a ferroelectric material whose dipole moments are largely dependent on temperature. In fact, based on material composition and dopant added, each PZT based ceramic has a pre-defined temperature at which material polarization will start to depole and piezoelectric effect will be lost. This temperature is called the Curie temperature, T_c.

Because of that phenomenon, PZT material design normally starts with selecting a composition with Curie temperature significantly above operating temperature, in order to ensure temperature stability and reliable functionality of PZT devices. Enhancing other materials properties such as the coupling factor, mechanical strength, or piezoelectric constant usually follows by further altering of composition and dopants used within the window of the accepted T_c range [5].

2.3.4 Manufacturing Method of Bulk PZT

The manufacturing process of PZT material starts with preparing the ceramic powder. In order to ensure reproducibility of material properties, powder particles shape, size and compositions should be uniform.

As illustrated in Figure 2-6, the manufacturing process of bulk PZT starts with the weighing of components to the right portions. After thorough mixing, ceramic powder is fired at 800-900 ^{o}C for 1-2 hours. The firing process is called the calcination process and it is when desired chemical composition is made. After that, ceramic powder is crushed and formed into the desired shape.

If more pure and uniform particles are required, the sol-gel method is introduced to the process. Sol-gel is steps 2 and 3 in figure 2-6. In this method, metal alkoxides are mixed in alcohol with the presence of water. Alcohol reacts with metal alkoxides to generate metal oxides in the form of a very fine and pure powder. The resulting powder is then put to calcination and the process continues as previously explained.

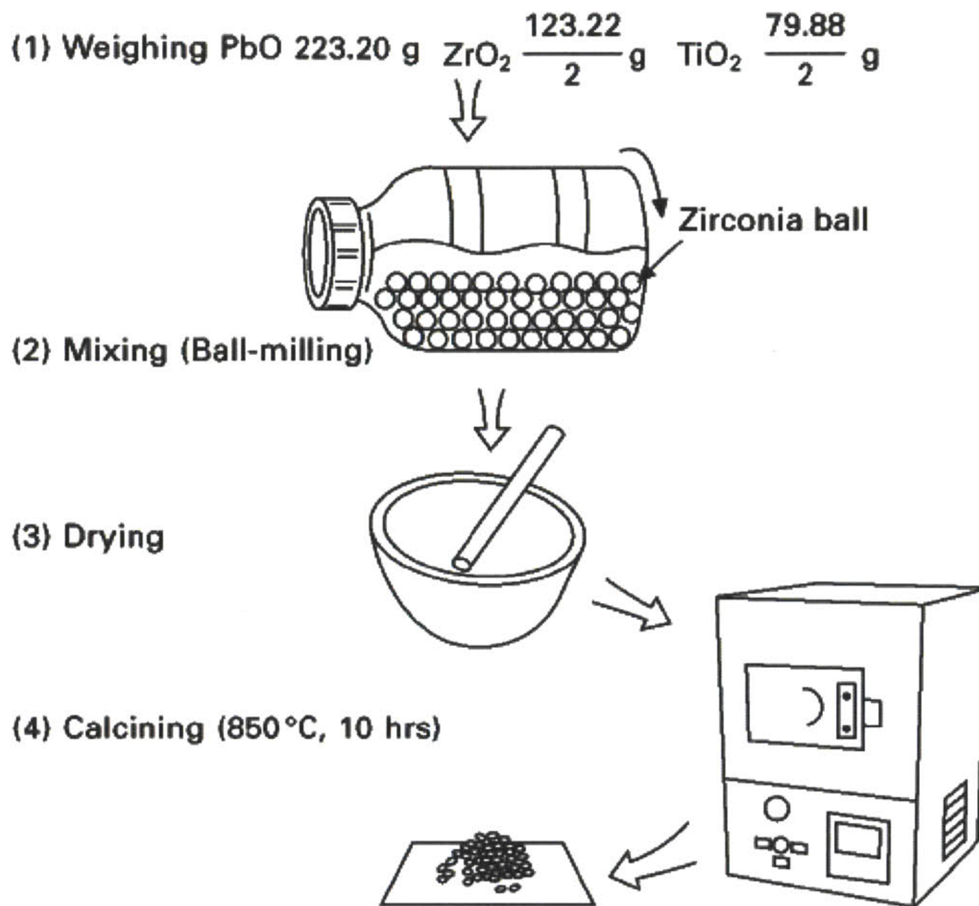

Figure 2- 6: $Pb(Zr_{0.5}Ti_{0.5})O_3$ powder preparation process [5].

PZT material preparation is followed by another process called sintering. In this step, shaped products are fired at a very high temperature that is slightly below melting temperature. During sintering, PZT grains grow in size and diffuse into adjacent grains as shown in Figure 2-7. The grains diffusion increases internal bonding and mechanical strength of the final product. It is also known that more sintering will produce bigger grains and ultimately a higher density PZT. Time dependent grain growth is illustrated in figure 2-8 [5].

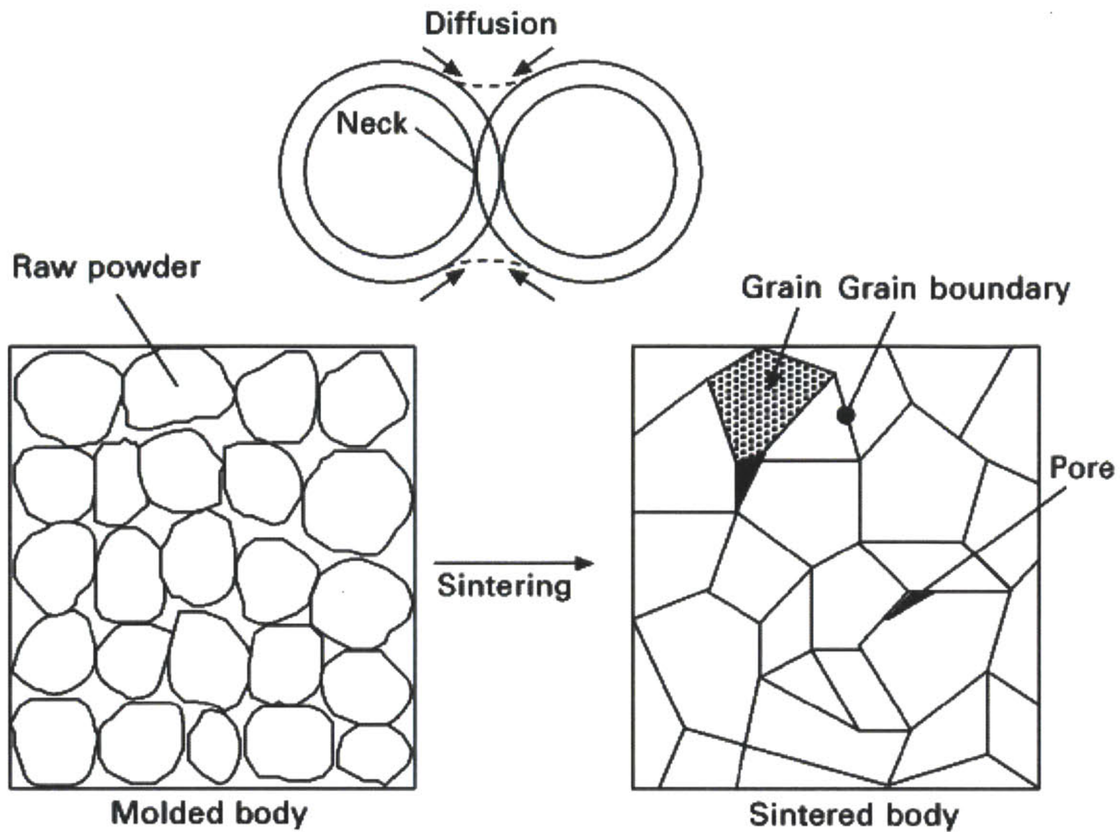

Figure 2- 7: Grain growth and diffusion during sintering [5].

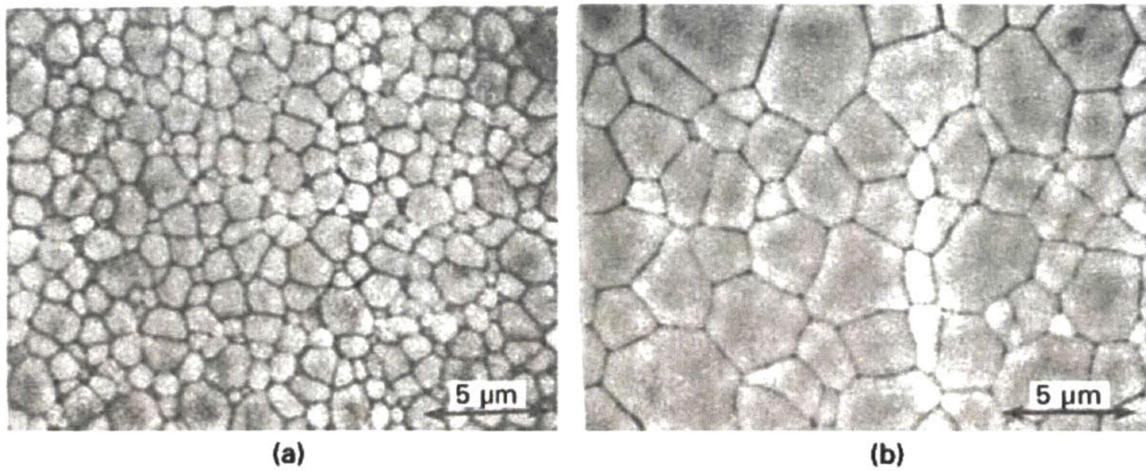

Figure 2- 8: Effect of sintering time on grain growth a) 1 hour and b) 16 hours [5].

2.4 Poling Process

Although PZT is a ferroelectric material and contains permanent intrinsic dipole moments at room temperature, net polarization is usually close to zero after sintering. This is explained by the randomness in the orientation of PZT dipole moments. Generally, a process called poling is required to reorient these moments in a single direction to establish the required overall polarization.

During poling, a very high voltage is applied to PZT wafers/substrates after being covered with a conducting electrode. As illustrated in figure 2-9, moments follow applied voltage direction. After the voltage is removed, some moments return to their original orientation, yet, most moments remain in the new orientation causing an increase in final polarization level. Remaining polarization is usually referred to as 'remanent polarization, P_r' [3].

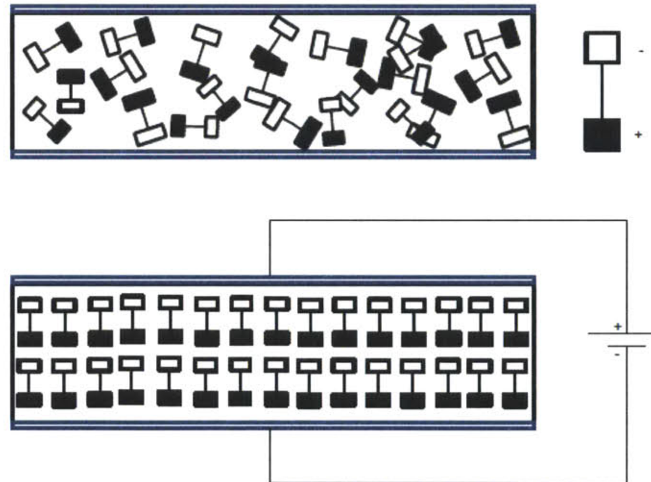

Figure 2- 9: Polarization of PZT.

The hysteresis loop shown in figure 2-10 is mostly used in literature to explain the polarization process of PZT. In that loop, point A represents the state of zero polarization. When the poling voltage is applied, polarization value follows the curve to point B where it reaches saturation.

When the voltage is removed, polarization level goes to remanent polarization value at point C [3].

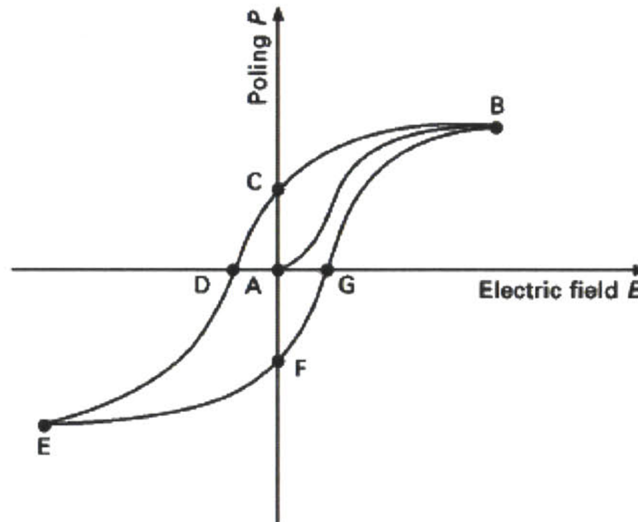

Figure 2-10: correlation between electric field E and polarization P [5].

2.4.1 Polarization Induced Stresses

During the poling process, internal strains and stresses are significantly increased because of the dipole moment reorientation that is taking place. The strain follows the butterfly curve shown in figure 2-11 as electric field is applied. Maximum strain values are seen at point B where poling voltage is also at maximum level. Most strain induced cracks that take place at poling happen around that point [5].

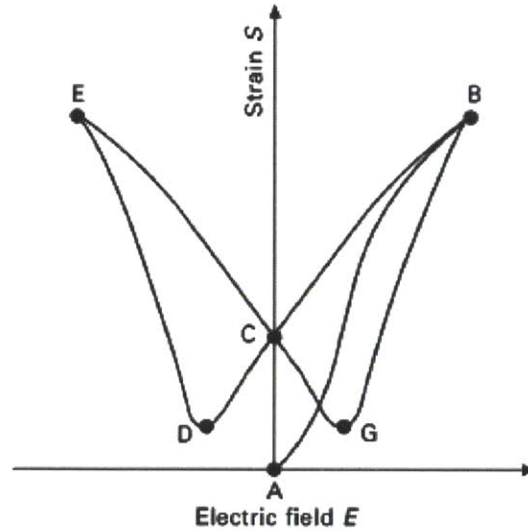

Figure 2-11: Correlation between electric field and strain [5].

2.4.2 Ions Doping and Poling

As stated in section 2.3.2, replacing some of the Pb^{2+} or Zr^{4+}/Ti^{4+} ions with lower charge ions in case of acceptor doping or with higher charge ions in case of donor doping has a direct effect in polarization process of PZT. This effect is summarized in figure 2-12.

For acceptor doping, some of the intrinsic dipole moments have a lower intensity because of the lower charge ions added. This fact will lead to an overall slower and less intense polarization at poling process. Higher electric field is required for achieving polarization saturation, yet, internal strains are building up at a milder base as well. This also has an effect in final product piezoelectric response that will be lowered.

Donor doping has an opposite effect because of the replacement of ions with higher charge. The polarization process is more rapid and is achieved with a lower voltage. The effect is more obvious for strain build up where a steeper increase is seen. The final product piezoelectric response is increased [5].

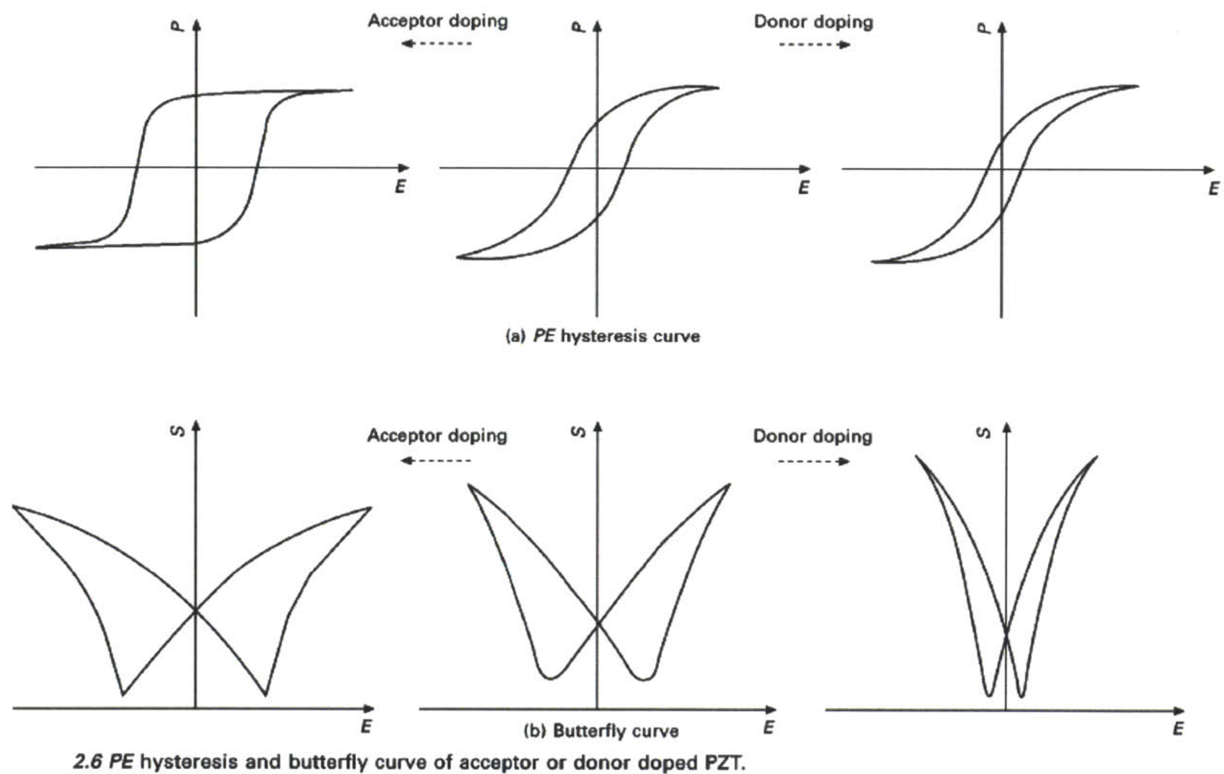

Figure 2- 12: Effect of acceptor and donor doping on PZT [5].

2.4.3 Liquid Dielectric and Poling

During poling of PZT substrates, high voltages are often applied between electrodes that are only a few microns apart. It is common to use dielectric fluids to prevent any voltage breakdown which is a phenomenon where insulating material will start to conduct electrical current. For example, the breakdown voltage of air is 7.6 kilovolts for a 2.4 millimeters (0.1 inches) gap. Breakdown voltage is commonly referred to as the dielectric strength [8].

Table 2.2 includes some of the dielectric fluids commonly used during poling, as well as their dielectric strengths [8-10]. The dielectric strength of air is included as a reference. Air is used as poling media in some of the experiments that will be discussed in later chapters.

Table 2- 2: Breakdown voltages for typical semiconductor industry dielectric fluid compared to air and vacuum

Material	Dielectric Strength (kV at 2.5 mm)
Air	7.6
Fluorinert Electronic Liquid FC-770	35
Fluorinert Electronic Liquid FC-40	46
Fluorinert Electronic Liquid FC-43	42
Novec 649	40
Silicon oil, Mineral oil	25.4-38.1

2.5 Sputtering Process

The sputtering process is a physical vapor deposition (PVD) technique that does not require high temperatures. In sputtering, inert gas particles are accelerated utilizing a very high voltage. These high energy particles are then directed into a direct collision with a target metal piece. This collision causes a release of some target atoms. These atoms fall into the wafer creating required metal layer.

This study requires knowledge of the specific path of trajectory for falling target atoms. In many cases, atoms take a straight path from target to substrate in what is known as the ballistic transportation. However, some of the low energy atoms released fall in a diffuse transportation trajectory. In diffuse transportation, atoms are transferred by collision with other atoms. They oscillate in the space between the metal target and the wafer while falling. This makes it very difficult to control falling atoms final location. The diffuse transportation of falling atoms leads to some contamination problems for the machine. The diffuse transportation also causes an incomplete shadowing of metal free areas of substrates or wafers [11]. Figure 2-13 illustrates this phenomenon.

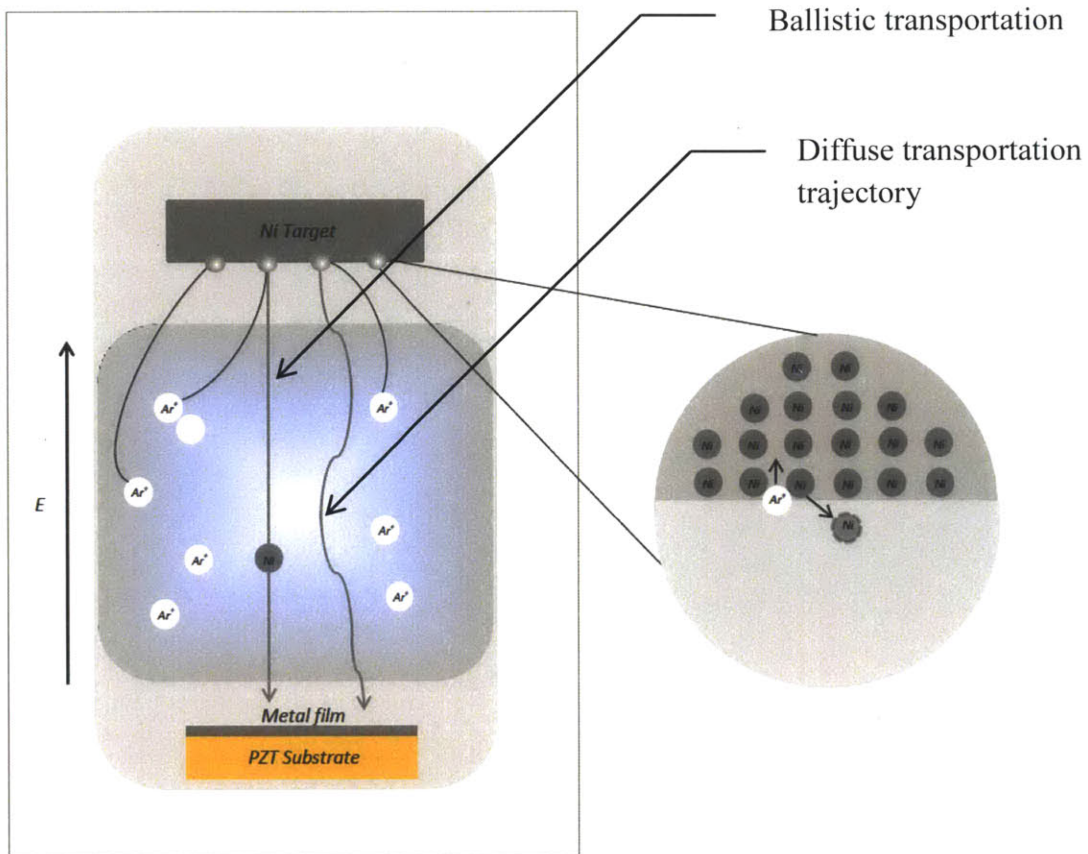

Figure 2-13: Ballistic and diffuse transportation trajectory during sputtering.

CHAPTER 3

Preliminary Analysis

This work focuses on the elimination of yield loss due to breakage of PZT substrates inside the poling machine, as indicated in Chapter 1. In this chapter, preliminary analysis of breakage during poling is presented. Based on this preliminary analysis, two possible causes of substrate breakage are suggested. These failure modes are:

- Electrical arcing between the two metal sides along the edges of PZT substrate due to metal overspray during sputtering.
- Intrinsic differential strains build up during poling due to the lack of complete metal coverage during sputtering.

3.1 PZT Substrate Breakage and Arcing

Observations indicated that poling breakage is always associated with electric arcing on the outer edges of PZT substrates. Figure 3-1 shows this phenomenon:

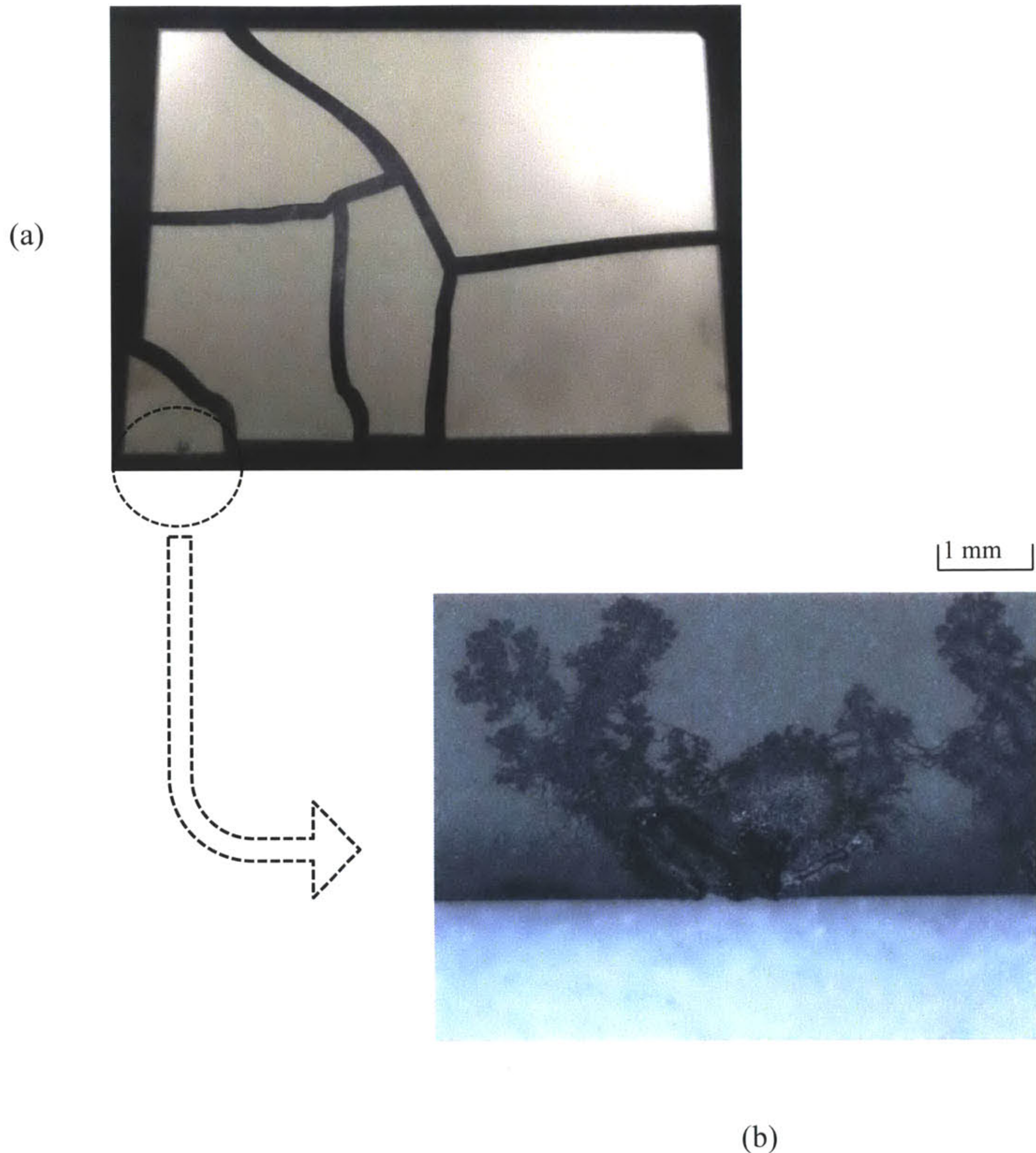

Figure 3-1: Substrate breakage and arcing; (a) substrate broken at poling; (b) magnified picture of arcing normally seen at substrate edges in case of breakage.

Electric arcing occurs along the edges in a way that suggests that an electrical current jump over is taking place. A flowery pattern is seen on both sides of substrates in case of arcing. It is believed that these flowery patterns are metal oxidation because of high temperature during arcing. Arcing typically happens at or close to maximum poling voltage.

Upon stripping metal using chemical etching, the arcs were found to have reached PZT material on both sides as shown in Figure 3-2:

Figure 3-2: Arcing marks reaching PZT material: a) arcing marks before etching; b) arcing marks on PZT material after etching.

3.2 Chemical Analysis

X-ray photoelectron spectroscopy (XPS) chemical analysis was conducted to identify the composition of the flowery pattern that is reaching PZT material as seen in Figure 3-2. The root of the burning marks was selected as Region 1 and a reference plane PZT region where no burning marks exist was selected as Region 2.

After performing the test, no significant composition difference in terms of lead, zirconium and titanium was observed. Also, no traces of nickel were available for Region 1. It was concluded that the heat generated by the electric arcing is actually burning the PZT material. This is believed to be assisting in breaking substrates during poling.

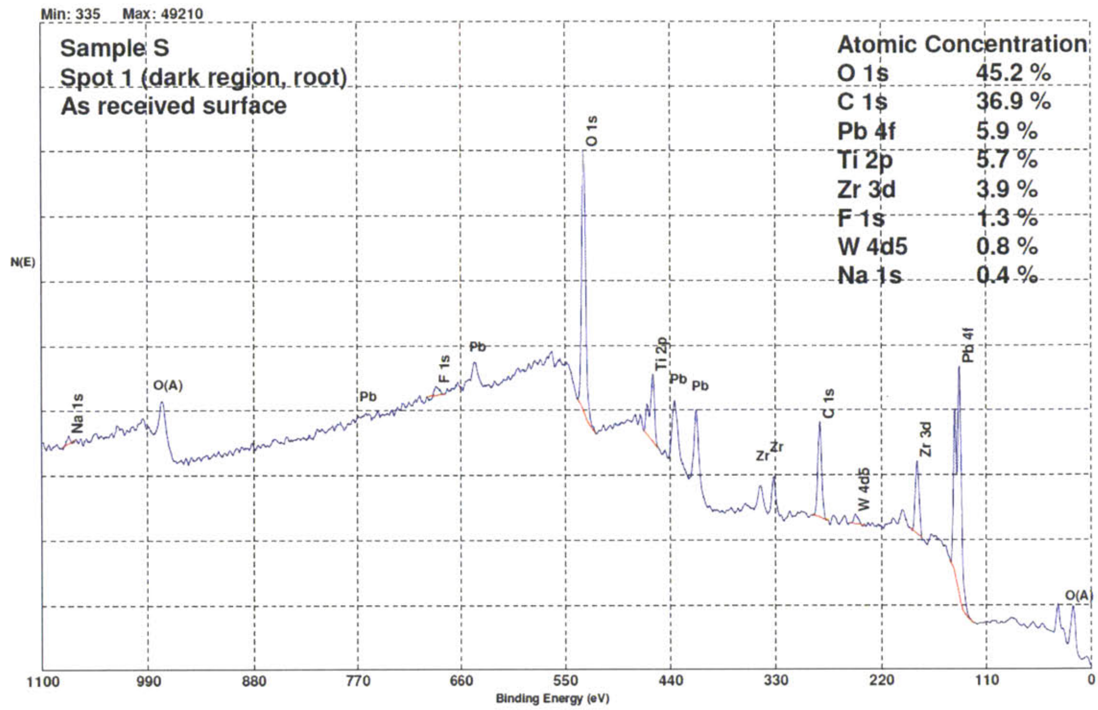

a)

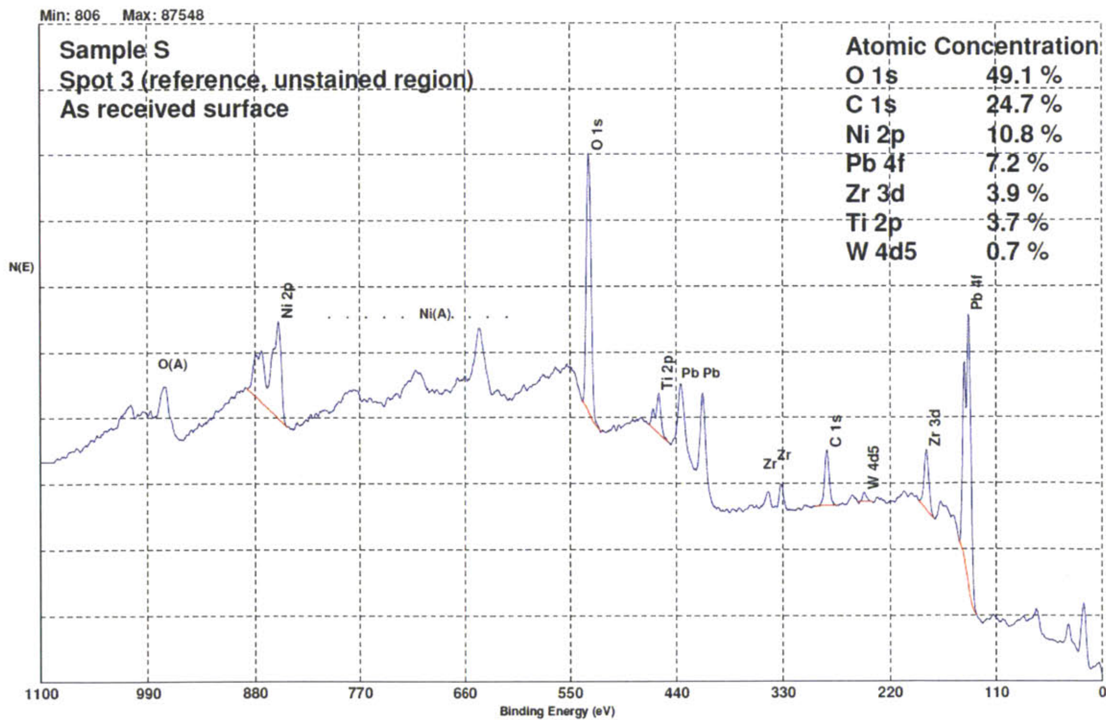

b)

Figure 3-3: Chemical analysis result a) Region 1: root; b) Region 2: reference material.

3.3 Inconsistency in Metal Coverage

Another important fact that was noticed with PZT substrates at poling is the inconsistency of metal coverage. Ideally, the PZT substrate outer frame should be metal free. The purpose of this metal free area along the substrate edges is to prevent any short circuit between the two metal sides during poling. However, it was noticed that substrate pattern side (8000 Angstroms Ni layer) is always covered completely with metal. It was found that Ni overspray is taking place while sputtering substrate pattern side causing the areas along the edges to be covered with nickel only. Figure 3-4 represents this inconsistency of metal coverage after sputtering.

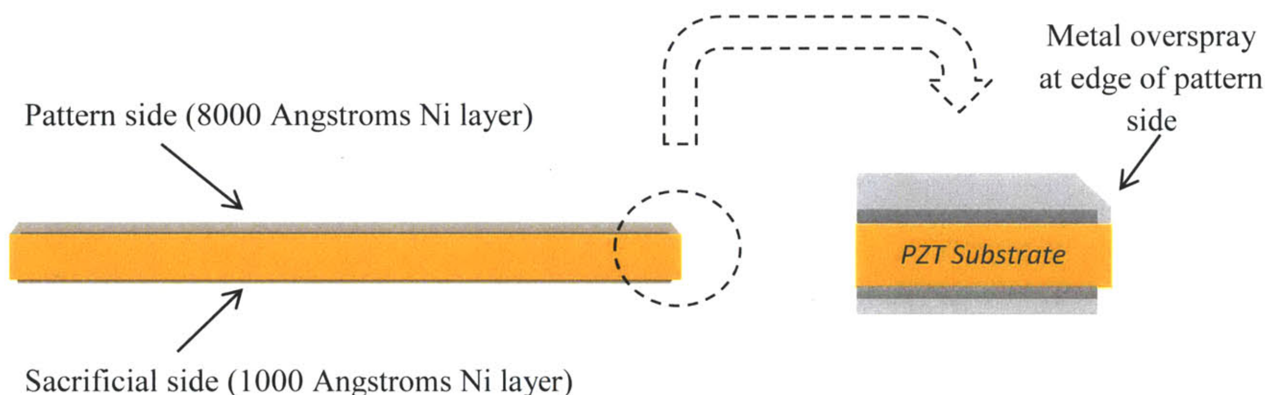

Figure 3-4: Inconsistency of metal coverage; Ni overspray on Pattern side.

It was concluded that this inconsistency in metal coverage is caused by insufficient metal shadowing at sputtering. In practice, a shadow mask, which is a fixture used to hold substrates in place during sputtering, is also supposed to control metal overspray. The depth of substrates inside the shadow mask, Z-direction in Figure 3-5, plays a crucial part in achieving that goal. Metal overspray is expected to take place if the substrate depth is not large enough inside the shadow mask. This was proven by a reverse sputtering experiment where the sacrificial side was sputtered using the 2 millimeters (0.08 inches) side of the shadow mask. Metal overspray was

seen with the sacrificial side instead despite the fact that nickel layer thickness is only 1000 Angstroms.

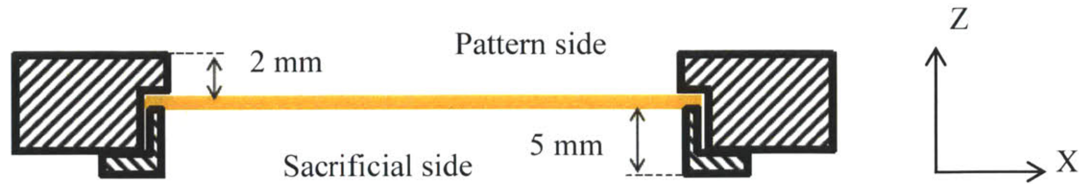

Figure 3-5: Substrates position inside shadow mask.

3.4 Potential Failure Modes

In light of the observations and results of the preliminary analysis conducted, the combination of the following two failure modes is believed to be causing breakage of substrates inside the poling machine:

- Electrical arcing between the two metal sides along PZT edge surface due to metal overspray.
- Intrinsic differential strains build up during poling due to lack of complete metal coverage during sputtering on substrate sacrificial side.

3.4.1 Electrical Arcing Due to External Nickel Overspray

As illustrated in Figure 3-6, Ni overspray during sputtering is suspected to be closing the 0.2 millimeters (0.008 inches) gap between the metal two sides. Closing this gap will reduce the breakdown voltage to levels below the initial 2.8 kilovolts for the used dielectric fluid. Any excessive metal overspray that reduces the gap between the two metal sides to 0.07 millimeters (0.0029 inches) or lower will cause an electric arcing during poling since breakdown voltage is reduced to values below poling voltage.

Figure 3-6: Nickel overspray during sputtering that might lead to arcing.

3.4.2 Intrinsic Differential Strains Build Up during Poling

During poling, PZT dipole moments follow applied voltage direction. The dipole moments expand in the direction of applied voltage causing a volumetric change in PZT substrate. In the poling process, the thickness increases slightly while total surface area decreases. This volumetirc change happens only in substrate areas that are covered with metal layer on both sides.

Hence, exposed areas experience low or zero reorientation and therefore low or zero strains. This difference in strain levels generates internal stresses in a plane perpendicular to substrate surface along the boarder between metal covered and metal free areas. These stresses are believed to be causing the poling breakage phenomenon if arcing is also present. The effect of the incomplete metal coverage during poling is illustrated in Figure 3-7.

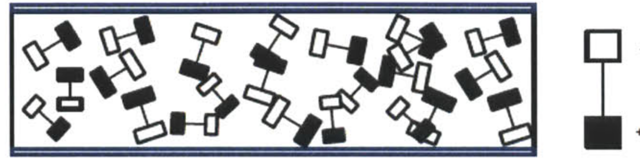

(a)

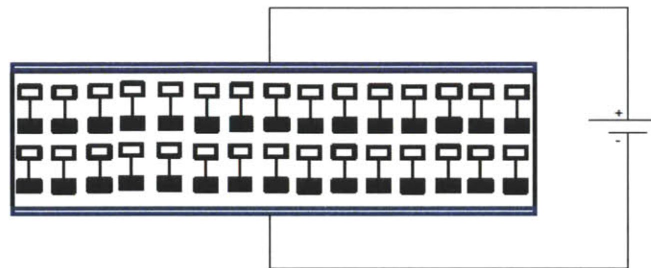

(b)

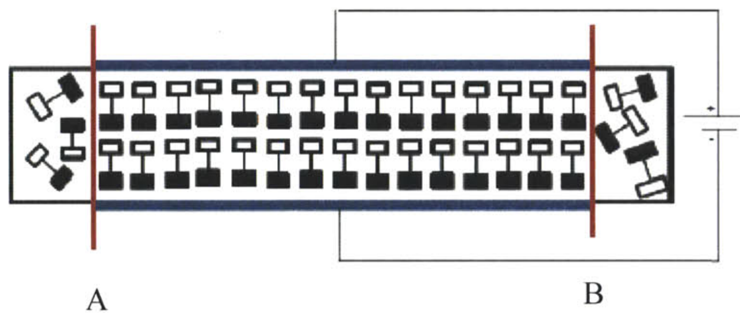

(c)

Figure 3-7: (a) dipole moments random reorientation before poling; (b) poling with complete metal coverage; dipole moments reorientation takes place for entire substrate; (c) poling with edges exposed generates stresses at plane A and B due to differential strains.

CHAPTER 4

Experimental Procedures

In this chapter, the experimental procedures followed to identify the root cause of substrates breakage will be explained. Two sets of experiments were designed and conducted to validate the two possible causes listed in Chapter 3.

Compared to other type of failures, poling breakage rarely takes place. In order to obtain conclusive results, altering of some process procedures and parameters was necessary to accelerate poling breakage. This was necessary to dilute any effect of process variation on the outcome of each experiment. The altered process step or parameter was selected carefully to affect investigated failure mode only. For example, when the effect of metal overspray on arcing and breakage was tested, no dielectric fluid was used during poling to stimulate arcing and breakage.

Experimental results were either compared to yield historical data or to the result of a control experiment where altered process parameter was kept unchanged. The scenarios included in each set of experiments are not sequential. The main metrics that were used for comparison were arcing and breakage counts.

4.1 Nickel Overspray

In this experiment, the effect of nickel overspray to the edges of substrates was investigated. For this experiment, no dielectric fluid was used during poling. As explained earlier, dielectric fluid is used to prevent any voltage breakdown between the two metal sides at high voltages which is the case with poling. Instead of using the dielectric fluid, substrates were poled in air. For a substrate thickness of 0.2 millimeters (0.008 inches), air breakdown voltage is around 600 Volts,

assuming full metal coverage from both sides of substrates and ignoring effect of electrode shape. Since poling voltage is 1000 Volts, arcing and breakage were expected to be increased significantly.

In this experiment, 42 substrates were poled in air with all other process parameters unchanged. Another 42 substrates were poled in air also but after mechanically removing any metal overspray traces off the edges using sand paper. An additional 42 substrates were also poled in air after chemically removing any metal overspray off the edges using an etchant bath. For the last experiment, substrates were spray coated with photoresist that was manually removed off the edges using Acetone. The substrates were then dipped into a metal etchant bath to completely remove any traces of metal off the substrate edges. Substrates were then poled after stripping photoresist.

Arcing and breakage counts were compared for the three scenarios. If metal overspray is really the root cause for arcing and breakage, then stripping the substrate edges off any metal traces is expected to decrease or eliminate poling arcing and breakage.

Settings are shown in table 4-1:

Table 4- 1: Nickel overspray experiment – no dielectric fluid

Experiment no.	Description	No. of subs	Expected result
1	Poled in air with no change in process	42	Increase in arcing and breakages
2	Mechanically removing nickel off edges	42	Decrease or eliminate arcing and breakages
3	Chemically removing nickel off edges	42	Decrease or eliminate arcing and breakages

4.2 Custom Imaging Mask

In this experiment, stress induced by the strain differences explained in the preliminary analysis was investigated. To do that, a special photoresist imaging mask was used. As shown in Figure 4-1, this mask is exposing a relatively big area around the edges of PZT substrates during imaging. The idea was to spray coat several substrates with photoresist and to chemically etch metal off substrates outer frame using etchant bath after removing photoresist from that area. This was expected to increase the suspected strain differences generated by the poling process.

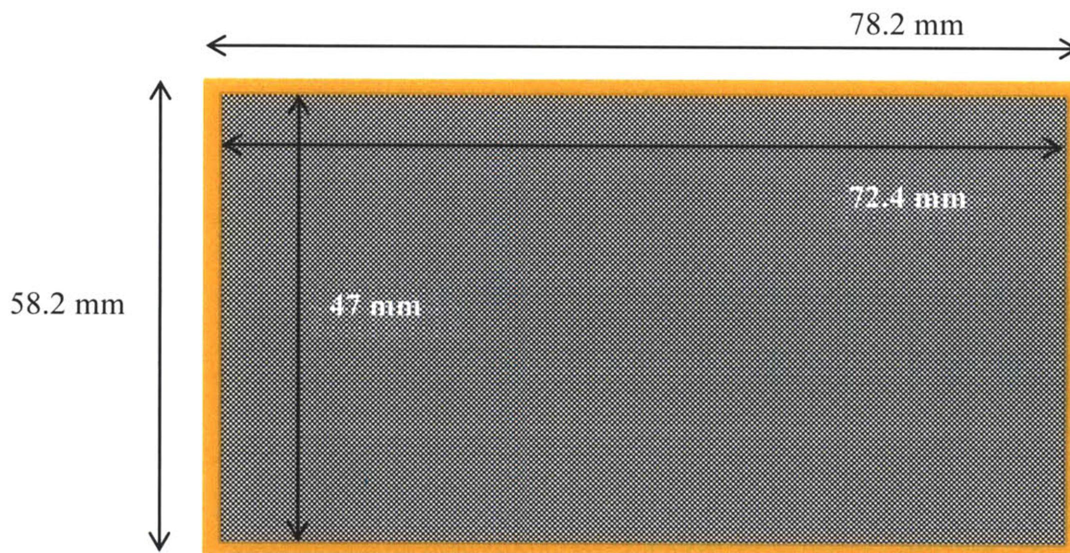

Figure 4-1: Custom imaging mask.

14 substrates were poled in air and tested for arcing and breakage. As a control experiment, another 14 substrates were sputtered with metal layer without the usage of shadow mask to have a complete metal coverage. This was expected to eliminate differential strains since dipole moment reorientation will be taking place for the whole substrate area equally.

Table 4-2 summarizes the different settings for this experiment:

Table 4-2: Custom imaging mask experiment – no dielectric fluid

Experiment no.	Description	No. of subs	Expected result
1	Etched metal outer frame	14	Increase in strain/stress that lead to breakages
2	Complete metal coverage	14	No strain/stress and no breakages

CHAPTER 5

Experimental Results and Discussion

After conducting the experiments explained in Chapter 4 and some follow up experiments, the following results were obtained:

- Conducting poling without the utilization of dielectric fluid caused an increase in arcing and breakage incidents. For the control experiment where 42 substrates were poled in air, arcing took place in 26% of the total substrates and 11% of substrates broke during the process.
- Mechanically removing suspected metal overspray by sanding caused an unexpected increase in arcing and breakage incidents, 36% arcing and 21% breakage.
- Chemically removing metal overspray experimentally decreased arcing and breakage by 80%; only one substrate broke during poling for this experiment.
- In the strain experiment, 100% breakage was encountered with substrates poled after etching outer frame. To the contrary, no breakage was found with substrates that were completely covered with metal layer despite the fact that arcing took place for 50% of total substrates.

5.1 Nickel Overspray

The hypothesis that metal overspray to edges during sputtering process is causing the poling arcing was tested in this experiment. For the three parts of this experiment stated in Section 4.1, possible arcing was stimulated by not using the dielectric fluid. If poling arcing incidents are reduced by removing suspected metal overspray mechanically or chemically, then this hypothesis is proven.

As shown in Table 5-1, poling without dielectric fluid caused an increase in arcing and breakage. In the first part of the experiment, ordinary substrates were poled without any additional change in the process. For these substrates, metal overspray was suspected to be reaching substrate edges. For this experiment, the arcing phenomenon took place in 26% of the 42 substrates and breakage was increased from a historical 2% to 11%.

In the second part of the experiment, arcing and breakage were expected to be reduced since traces of metal overspray were removed mechanically using sand paper. However, this experiment resulted in an increase in arcing and breakage counts compared to the first part of the experiment. Arcing and breakage as seen in Table 5-1 were 36% and 21%, respectively. Two things were taking place. First, metal removal was not appropriate as leftover metal on sand paper was sticking back to substrate edges. Second, as illustrated in Figure 5-1, the distance between metal layer and substrate edge for the sacrificial side was getting shorter due to the sanding of some of the PZT material. This resulted in a shorter gap between the two metal sides and an increase in arcing and breakage.

Figure 5-1: Reduction of distance between metal sides after sanding edges; (a) initial space between metal sides; (b) effect of removal of PZT material and the reduction in space between metal sides.

For the third part of this experiment, traces of metal overspray were chemically removed using an etchant bath. This reduced arcing and breakages from 26% and 11% to 2%, as seen in Table

5-1. Here, PZT substrate original dimensions were maintained and removing of metal traces off substrate edges was almost perfect.

It was proven in this experiment that arcing is indeed caused by the metal overspray phenomenon. It was also shown that breakage during poling is increased by the increase in arcing.

Table 5-1: Nickel overspray experiment results

Experiment no.	Description	No. of subs	Result
1	Poled in air with no change in process	42	26% arcing and 11% breakages
2	Mechanically removing nickel off edges	42	36% arcing and 21% breakages
3	Chemically removing nickel off edges	42	2% arcing and 2% breakages

5.1.1 Reverse Sputtering

An additional experiment was conducted based on the result of the overspray experiment and dependence of metal overspray on the duration and depth of the PZT substrate inside the sputtering shadow mask. As explained in Section 3.3, one cause of metal overspray for the 8000 Angstroms side is the small depth inside the shadow mask and the longer period it takes to finish sputtering for this side compared to the 1000 Angstroms side.

In this follow up experiment, 54 substrates were poled without using the dielectric fluid after a reverse sputtering was done. In reverse sputtering, the 8000 Angstroms side was sputtered with the deeper side of the shadow mask and the 1000 Angstroms side was sputtered with the shallower side as seen in Figure 5-2. Reverse sputtering resulted in a less covered pattern side as the depth was 5 millimeters compared to 2 millimeters. Also, the sacrificial side was not

completely covered with metal because of the shorter time it takes to sputter the 1000 Angstroms thickness metal layer relative to that of the 8000 Angstroms.

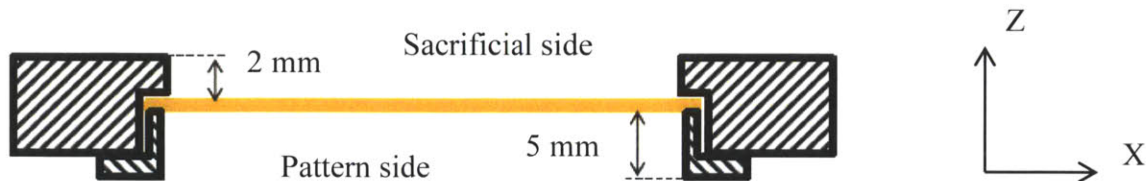

Figure 5-2: Reverse sputtering experiment: pattern side is coated with metal using the deeper side of the shadow mask instead of the shallower side.

In this follow up experiment, arcing and breakage happened only for 3.6% of the total substrates. Compared to the first part of this experiment, reverse sputtering resulted in a reduction in arcing and breakage by 22.4% and 7.4%, respectively.

The shadow mask design effect was significantly highlighted in this experiment. It is concluded from this experiment that metal overspray is significantly reduced if the depth of the substrate inside the shadow mask is increased.

5.1.2 Low Poling Voltage

Another additional experiment was done to identify at which voltage level arcing will stop taking place if substrates were to be poled without using the dielectric fluid. Poling voltage was reduced in 100 Volts increments until arcing stopped taking place. It was found that no arcing occurred when voltage was reduced to 500 Volts. The effect of lowering the poling voltage on arcing is another evidence that arcing is directly related to current jump over due to high voltage during poling. This experiment suggests also that lowering poling voltage or using a dielectric fluid with

higher breakdown voltage will improve the situation as far as arcing and poling breakage are concerned. In addition to that, differential strains along edges of substrates will be lower since less polarization will be achieved at a poling voltage of 500 Volts as opposed to 1000 Volts. For this experiment, final capacitance value and capacitance increase percentage were measured and calculated and they were found in compliance with final product requirements.

5.2 Custom Imaging Mask

A custom imaging mask was designed to test if the intrinsic stresses due to differential strains along substrate edges are really contributing to the poling breakage problem. It has been considered that the lack of metal coverage along the edges is causing some degree of differential strains that induces stresses. To aggravate this suspected effect, this metal free area was enlarged using the experimental procedure explained in Section 4.2. The poling breakage result of this experiment was compared to the second type of substrates where metal coverage was perfect; substrates sputtered without the usage of a shadow mask.

As shown in Table 5-2, enlarging the metal free area along the edges resulted in 100% breakage; yet, no arcing was noticed. For the second part of the experiment, although arcing was taking place for 50% of the total substrates, no breakage was seen.

According to these results, it is shown that the effect of differential strain and stresses along substrate edges is highly significant if the metal free area is large enough. Also, it was shown that arcing might take place without any breakage if a perfect metal coverage is assured where intrinsic stresses are eliminated. It was concluded from this experiment that arcing is not the sole cause of the poling breakage. Instead, some degree of internal stresses along substrate edges must be present for a breakage to take place during poling.

Table 5-2: Custom imaging mask experiment results

Experiment no.	Description	No. of subs	Result
1	Etched metal outer frame	14	100% breakage with no arcing
2	Complete metal coverage	14	Zero breakage with 50% arcing

5.2.1 Custom Imaging Mask Follow Up Experiment

To further validate these findings, an additional experiment was conducted where metal was removed from an area at the middle of the substrate instead of the outer frame of the substrate. This substrate was poled using the dielectric fluid and it still broke during poling. Another substrate where edges were cleared of any metal was also poled using the dielectric fluid and breakage was encountered. This eliminates the effect of dry poling. Figure 5-3 shows pictures of two substrates broken in this experiment. It is clear that the breakage was initiated at the metal free areas for both cases.

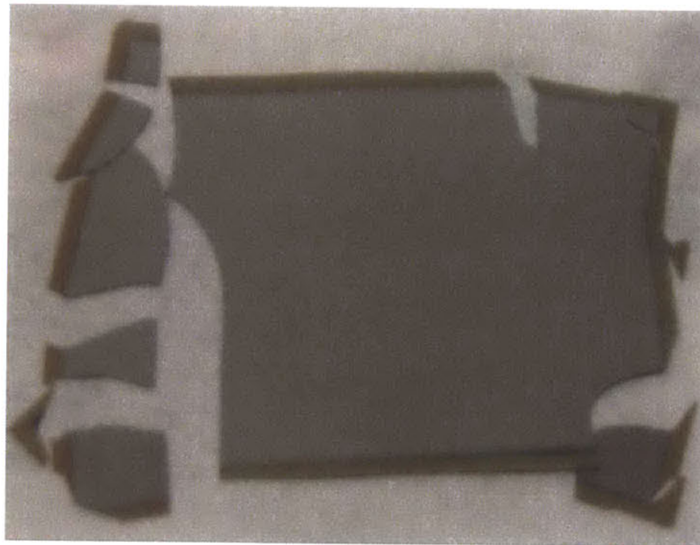

a)

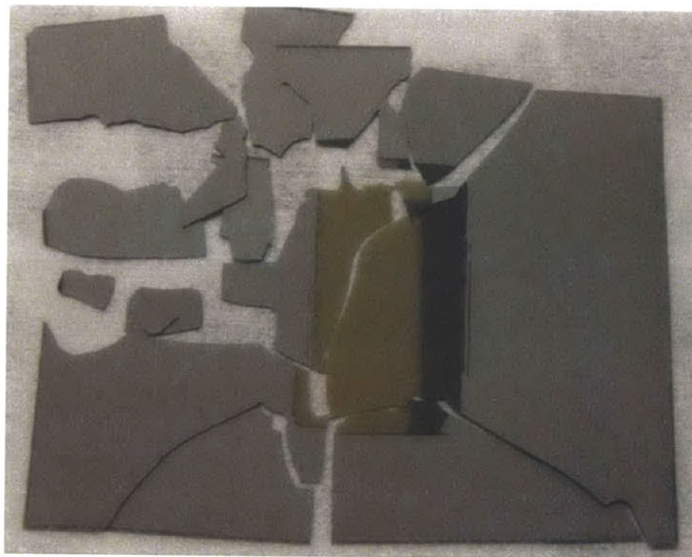

b)

Figure 5-3: Differential strains experiment; a) outer frame free of metal coverage; b) middle area free of metal.

5.3 Upgraded Sputtering Shadow Mask Design

Based on the results from the reverse sputtering experiment, an upgraded design of the existing sputtering shadow mask was suggested. Previous results showed that metal overspray was significantly reduced when the deeper side of the shadow mask is used during sputtering. Based on that fact, a proposed experimental shadow mask was design to have an even depth of 5 millimeters on both sides. All other old mask dimensions were kept unchanged. Figure 5-4 is an illustration of the new mask.

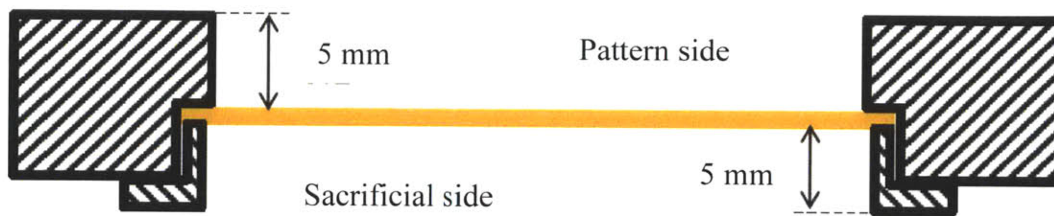

Figure 5-4: Trial shadow mask with even depth for both sides.

This shadow mask was used to sputter 42 substrates. An almost metal free frame was noticeable for all substrates as shown in Figure 5-5. These substrates were poled without the use of dielectric fluid. This experiment resulted in 2.4% arcing and breakage. This is a better result than the simple reverse sputtering experiment included in Section 5.1. Adopting this upgraded shadow mask is expected to completely eliminate the poling breakage phenomenon if implemented at a large scale with the usage of the dielectric fluid.

It was also noticed in this experiment that 5 substrates contained broken edges directly after sputtering. This might be solely related to some deviation in the sputtering process as frequently seen. It might also be due to the effect of achieving a perfectly metal free area during sputtering. Further testing is suggested using the new shadow mask. If the edge breakage continues, the depth of the shadow mask can be decreased and therefore increase the metal coverage toward the

substrate edges. The mask design could also be revised to reduce substrate shadowed area to achieve more metal coverage.

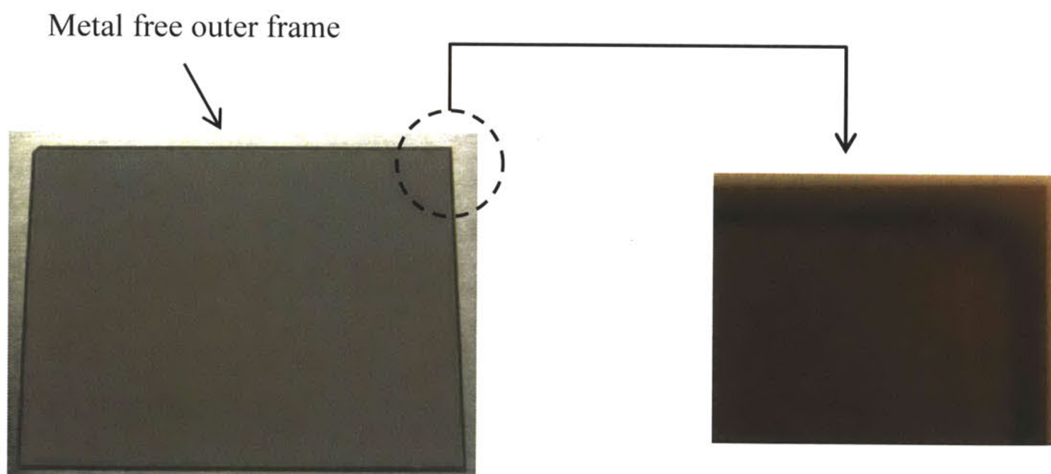

(a)

Metal covering all substrate area

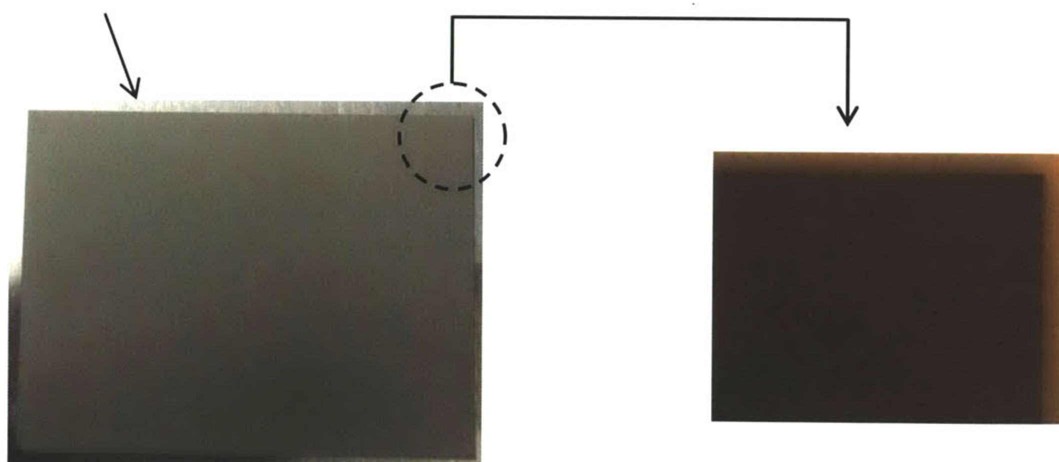

(b)

Figure 5-5: Effect of new shadow mask on metal overspray: (a) Substrate coated using new shadow mask showing metal free outer frame; (b) substrate coated using old shadow mask showing full metal coverage for pattern side.

CHAPTER 6

Conclusions, Recommendations and Future Work

The main objective of this thesis was to increase the process yield by 2% by eliminating the poling breakage defect type. The work included in this thesis showed that achieving this goal is possible. The poling breakage phenomenon root causes were successfully identified and validated by the nickel overspray experiment and the custom imaging mask experiment discussed in Chapter 4 and Chapter 5. The main conclusions highlighted in this thesis are:

- Frequently encountered substrate breakages during poling are caused by a combination of the differential strain build up along the edges and the shock wave generated by the poling arcing. The difference in strains along the edges makes the metal free area severely stressed and more susceptible to breakage if any form of mechanical force or shock is present during poling.
- Electrical arcing or current jump over between substrates metal sides is caused by the metal overspray during sputtering. Metal overspray is taking place due to a shadow mask design that does not completely prevent metal sputtered atoms from reaching substrate edges.
- Metal overspray shortens the distance between the two metal sides to a distance where a voltage breakdown is possible.

The upgraded shadow mask significantly decreased the metal overspray. The poling breakage was experimentally reduced by 70% under aggravated conditions; no dielectric fluid was used. It is believed that using the new design for mass scale production will lower poling breakages even

further. Nevertheless, following recommendations should be implemented before adopting the new shadow mask design:

- Test the experimental shadow mask on a larger scale focusing on arcing, breakage, and effect of new design on edges breakage during the sputtering process. Test lots shall be processed fully to identify any effect of the new design on final devices quality and overall process yield.
- If edges breakage continues to be an issue, consider machining the experimental shadow mask to decrease depth on both sides. Having a shallower shadow mask will reduce the metal free area along substrate edges. This should be done in increments as a part of a DOE to achieve optimal results. A proposed DOE is included in Appendix A.
- Another approach to reducing the metal free area along substrate edges is to reduce substrate shadowed areas by upgrading existing shadow mask design. Revision of used shadow mask dimensions is included in Appendix B.

Also, several possibilities for future work could improve the process further:

- Evaluate the effect of metal free area along substrate edges on the handling breakage. As mentioned, stresses along the edges are high because of the differential strains. This phenomenon might be related to the corner handling breakage seen in the process. Shadow mask design could be further revised to maximize metal coverage while preventing metal overspray to edges at the same time. A proposed new design is included in appendix B.
- Evaluate the possibility of reducing the poling voltage to a lower value. This will definitely reduce poling arcing and breakage
- Investigate the effect of the shadow mask design on the sputter arcing phenomenon.
- Study the effect of grounding the shadow mask and substrates during sputtering on sputter arcing phenomenon. Wafers and substrates are typically grounded during sputtering to release any charge build up.
- Redesign shadow mask used for other PZT products to eliminate excessive metal overspray that frequently requires edges sanding to perform the poling process. This will eliminate both: breakage during sanding and breakage during poling.

- Investigate the feasibility of utilizing a stronger dielectric fluid with a higher breakdown voltage.

APPENDIX A

Design of Experiment for Optimal Shadow Mask Design

Further testing of the new experimental shadow mask design should be conducted. This is to further evaluate the new design effect on the poling breakage, the broken edges issue that was noticed directly after sputtering, and the final process yield. If the broken edges issue continues to exist, one of the two proposed solution included in this appendix or in Appendix B could be followed. The two suggestions are directed to reducing the metal free areas around substrates' edges. Having more metal coverage is believed to be the solution to this problem.

One way to achieving more metal coverage is by reducing the depth of substrates inside the sputtering shadow mask. Below DOE could be followed to investigate the effect of reducing the substrates depth on the poling breakage and the broken edges phenomenon.

Experiment no.	Pattern side depth	Sacrificial side depth	No. of subs	Poling Breakage	Sputtering broken edges
1	4.3 mm (0.17")	4.3 mm (0.17")	42		
2	3.8 mm (0.15")	3.8 mm (0.15")	42		
3	3.0 mm (0.12")	3.0 mm (0.12")	42		
4	2.5 mm (0.10")	2.5 mm (0.10")	42		

Note:

- A very small gap should be maintained between substrates and shadow mask frames/caps.
- Dielectric fluid is not used in these experiments
- If experiment 4 generates the best results in terms of metal overspray and poling breakage, then the major factor that affects metal overspray is the gap between substrates and sputtering target and not the depth of substrate inside shadow mask.

APPENDIX B

Revision of Existing Shadow Mask Design

Another way of achieving more metal coverage is by redesigning the existing shadow mask to have a bigger exposed substrate area during sputtering. Suggested revision of existing shadow mask dimensions is indicated in the drawings below:

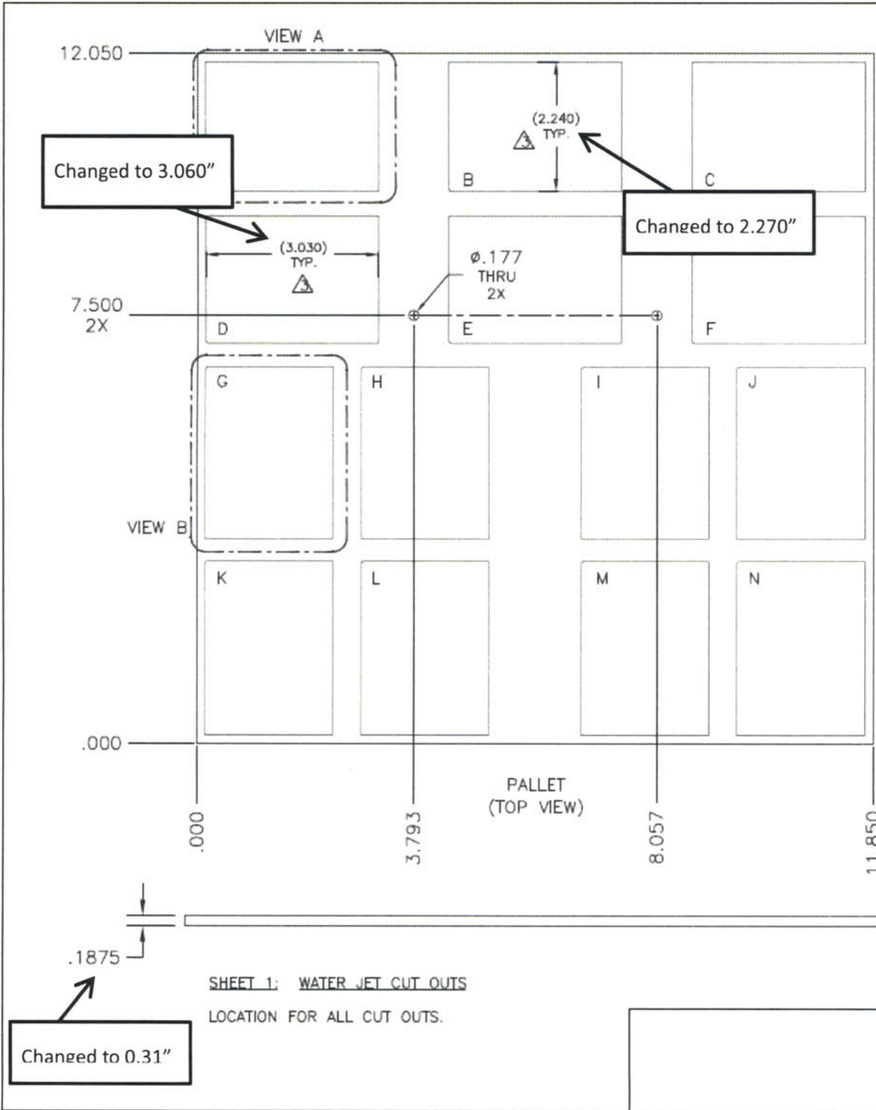

TABLE 1:

ORIENTATION	CUT THRU	ORIGIN X	ORIGIN Y
HORIZONTAL	A	0.145	9.696
HORIZONTAL	B	4.410	
HORIZONTAL	C	8.675	
HORIZONTAL	D	0.145	7.041
HORIZONTAL	E	4.410	
HORIZONTAL	F	8.675	
VERTICAL	G	0.176	6.595
VERTICAL	H	2.906	
VERTICAL	I	6.766	
VERTICAL	J	9.496	
VERTICAL	K	.0176	3.175
VERTICAL	L	2.906	
VERTICAL	M	6.766	
VERTICAL	N	9.496	

CUT OUT: 3.060" X 2.270 " THRU

DATE: 3/10/11			
BY:			
ALL DIMENSIONS ARE IN INCHES	SHADOW MASK SMALL BLANK PZT		SCALE: NONE
TOLERANCES UOS. XX±.01 XXX±.0025 XXXX±N/A	DWG NO. 10262-200	REV. B	SHEET: 1 of 6

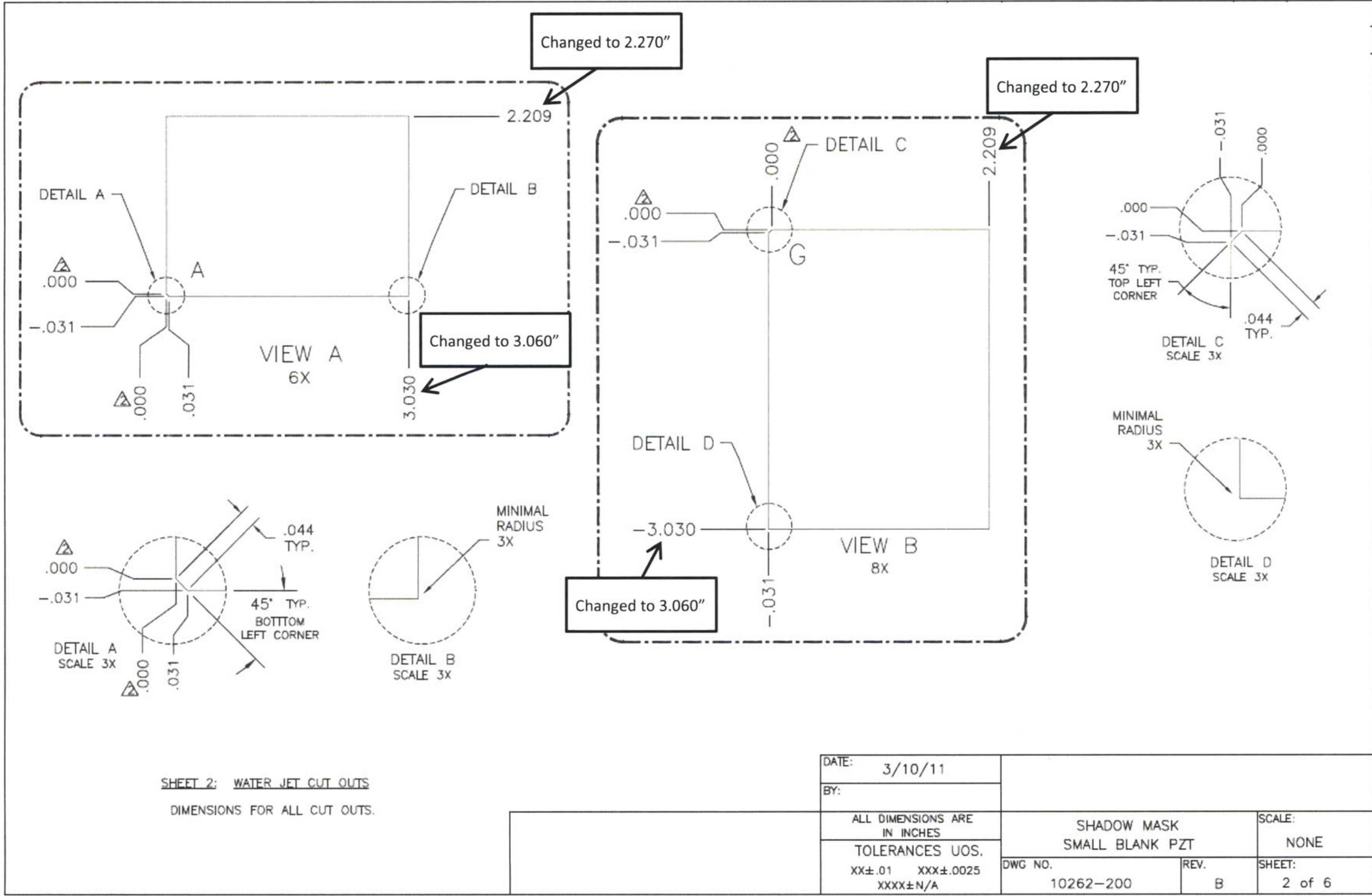
Changed to 2.270”
Changed to 2.270”
Changed to 3.060”
Changed to 3.060”
2.209
DETAIL A
DETAIL B
A
.000
-.031
VIEW A
6X
.000
.031
3.030
DETAIL C
.000
2.209
.000
-.031
G
DETAIL D
-3.030
VIEW B
8X
-.031
-.031
.000
.000
-.031
45° TYP. TOP LEFT CORNER
.044 TYP.
DETAIL C SCALE 3X
MINIMAL RADIUS 3X
DETAIL D SCALE 3X
.044 TYP.
.000
-.031
45° TYP. BOTTTOM LEFT CORNER
DETAIL A SCALE 3X
.000
.031
MINIMAL RADIUS 3X
DETAIL B SCALE 3X
SHEET 2: WATER JET CUT OUTS
DIMENSIONS FOR ALL CUT OUTS.
DATE: 3/10/11
BY:
ALL DIMENSIONS ARE IN INCHES
TOLERANCES UOS.
XX±.01 XXX±.0025
XXXX±N/A
SHADOW MASK
SMALL BLANK PZT
SCALE: NONE
DWG NO. 10262-200
REV. B
SHEET: 2 of 6

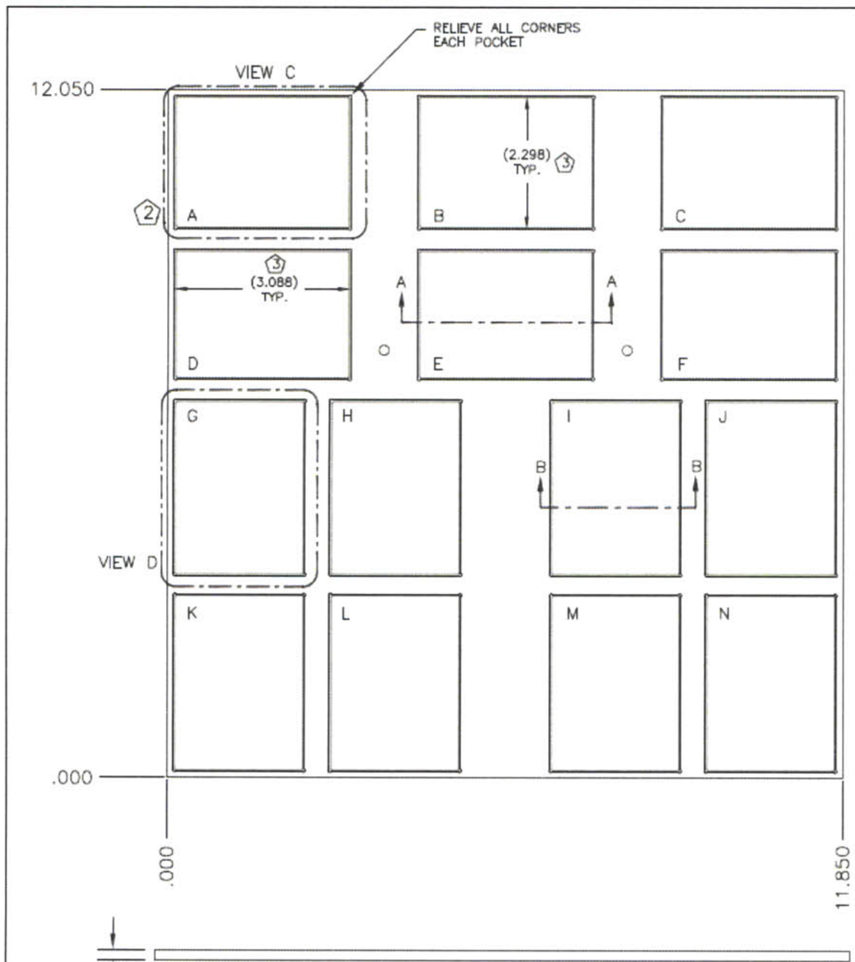

Changed to 0.31"

2

TABLE 2:

ORIENTATION	POCKETS	ORIGIN X	ORIGIN Y
HORIZONTAL	A	0.116	
HORIZONTAL	B	4.381	9,636
HORIZONTAL	C	8,646	
HORIZONTAL	D	0.116	
HORIZONTAL	E	4.381	6,981
HORIZONTAL	F	8,646	
VERTICAL	G	0.116	
VERTICAL	H	2,846	
VERTICAL	I	6,706	6.624
VERTICAL	J	9.436	
VERTICAL	K	0,116	
VERTICAL	L	2,846	3.204
VERTICAL	M	6.706	
VERTICAL	N	9,436	

SHEET 3: MACHINED POCKETS

LOCATION FOR ALL POCKETS.

DATE: 3/10/11	
BY:	
ALL DIMENSIONS ARE IN INCHES	SHADOW MASK SMALL BLANK PZT
TOLERANCES UOS. XX±.01 XXX±.0025 XXXX±N/A	DWG NO. 10262–200

SCALE:	REV.	SHEET:
NONE	B	3 of 6

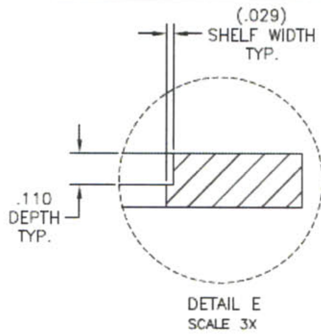

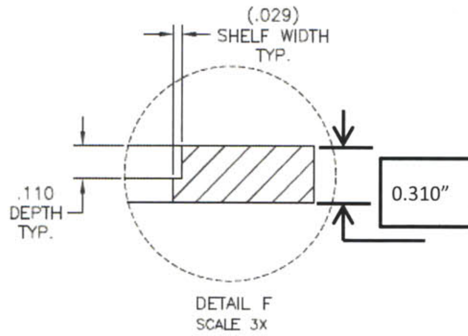

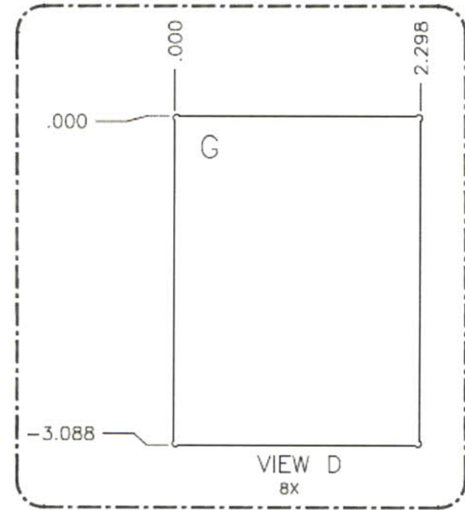

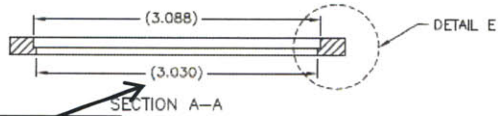

Changed to 3.060"

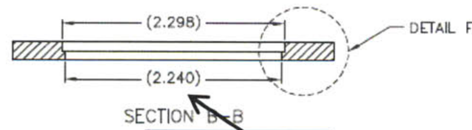

Changed to 2.270"

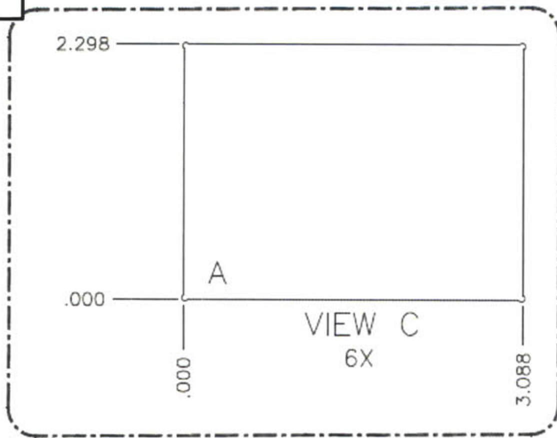

SHEET 4: MACHINED POCKETS

DIMENSIONS I

DATE: 3/10/11			
BY:			
ALL DIMENSIONS ARE IN INCHES	SHADOW MASK SMALL BLANK PZT		SCALE: NONE
TOLERANCES UOS. XX±.01 XXX±.0025 XXXX±N/A	DWG NO. 10262–200	REV. B	SHEET: 4 of 6

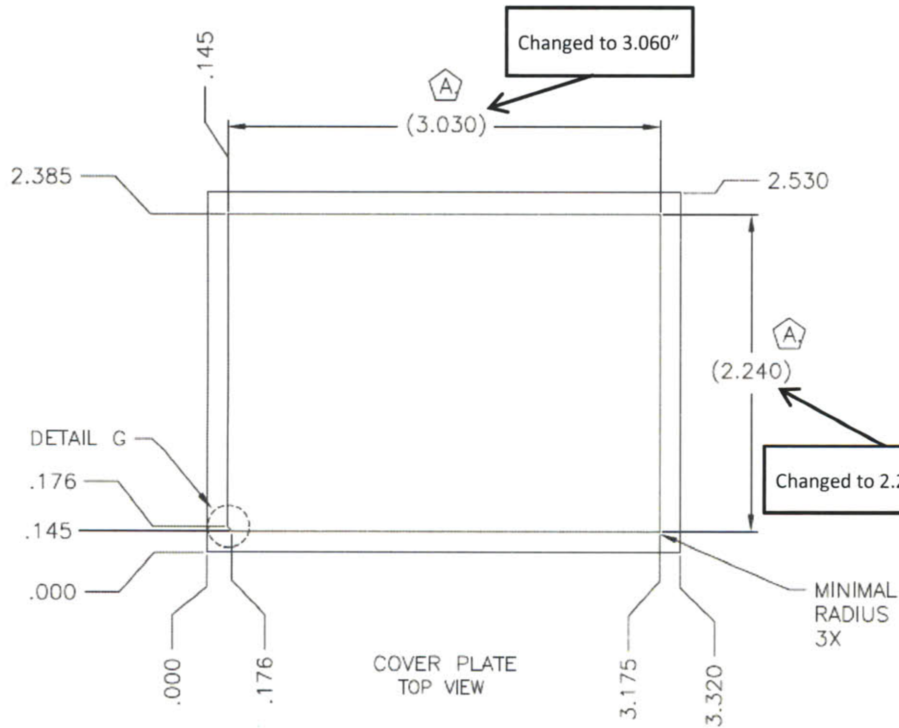

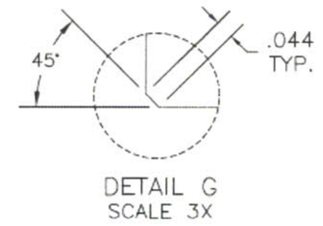

NOTES: ITEM 2: COVER PLATE QTY. 14 per PALLET

Changed to 0.31”

SHEET 5: WATER JET CUTOUT
DIMENSIONS FOR THE CUTOUT

DATE: 3/10/11	
BY:	
ALL DIMENSIONS ARE IN INCHES	SHADOW MASK SMALL BLANK PZT
TOLERANCES UOS.	SCALE: NONE
XX±.01 XXX±.0025 XXXX±N/A	DWG NO. 10262–200 / REV. B / SHEET: 5 of 6

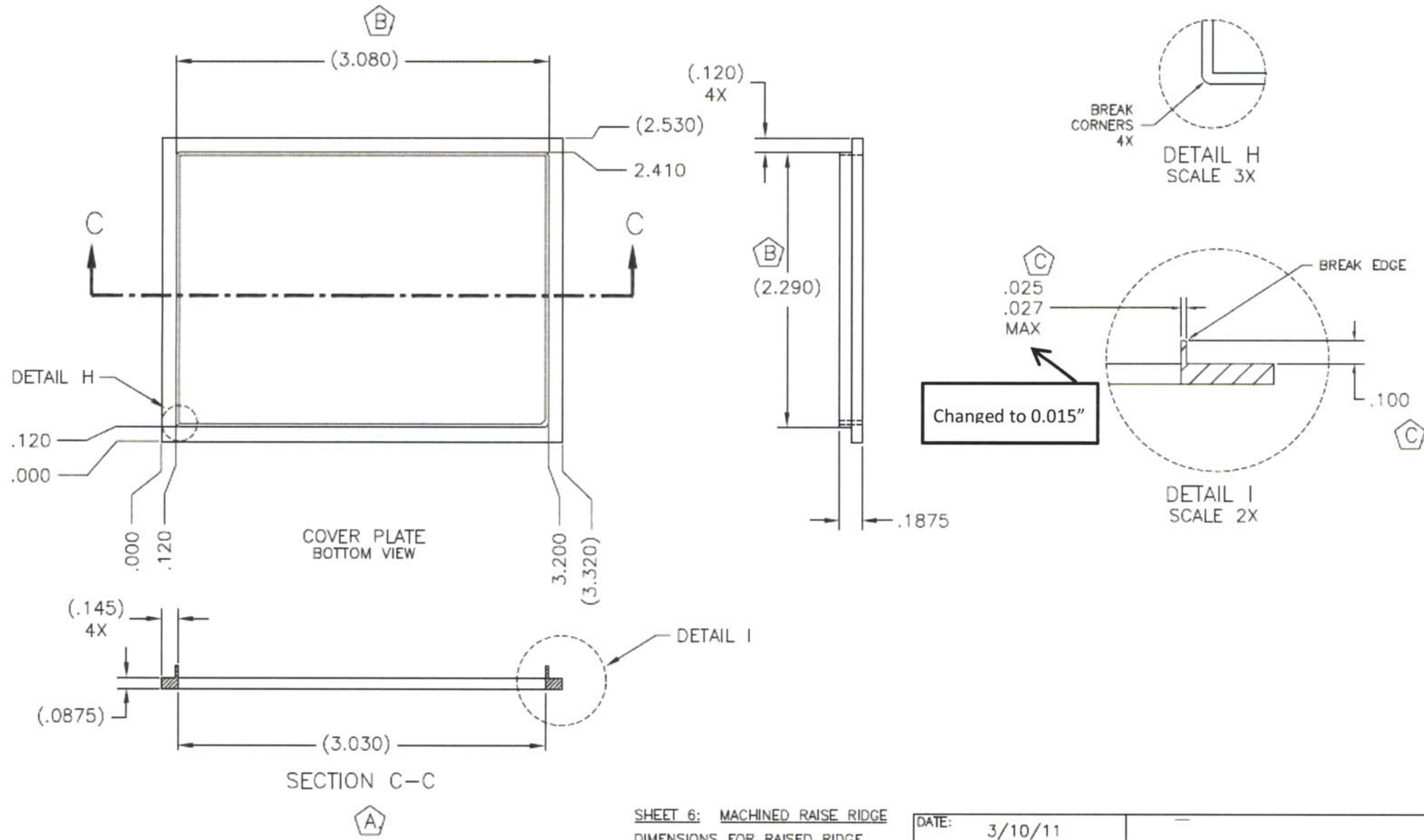

SHEET 6: MACHINED RAISE RIDGE
DIMENSIONS FOR RAISED RIDGE

DATE: 3/10/11	
BY:	
ALL DIMENSIONS ARE IN INCHES	SHADOW MASK SMALL BLANK PZT
TOLERANCES UOS. XX±.01 XXX±.0025 XXXX±N/A	DWG NO. 10262–200

SCALE:	REV.	SHEET:
NONE	B	6 of 6

REFERENCES

[1] Lee, J., 2012, "Determining the Root Causes of Excess Metal and Void Defects With Respect to the Photoresist Quality in Thin Film PZT Fabrication Processes" Master's thesis, MIT, Cambridge, MA.

[2] Dave, N., 2012, "Removal of metal oxide defects through improved semi-anisotropic wet etching process" Master's thesis, MIT, Cambridge, MA.

[3] Defay, E., 2011, *"Integration of ferroelectric and piezoelectric thin films: concepts and applications for microsystems"* ISTE, London; Wiley, Hoboken, NJ, Chap. 1.

[4] Hajati, A., 2010, "Ultra Wide-Bandwidth Micro Energy Harvester" Ph.D. thesis, MIT, Cambridge, MA.

[5] Uchino, K., 2010, *"Advanced piezoelectric materials: science and technology"* Woodhead Publishing, Cambridge, U.K., Chap. 2 & 10.

[6] Bathurst, S., 2008, "Direct Printing of Lead Zirconate Titanate Thin Films" Master's thesis, MIT, Cambridge, MA.

[7] Okuyama, M., Ishibashi, Y., 2005, "Ferroelectric thin films: basic properties and device physics for memory applications" Springer, Berlin; New York, pp. 127.

[8] "Dielectric Strength" April, 2012, [online]. Available: http://en.wikipedia.org/wiki/Dielectric_strength

[9] 3M Specialty Fluid, "Fluorinert™ Electronic Liquids for Electronic Reliability Testing" 1999, [online]. Available: http://multimedia.3m.com/mws/mediawebserver?mwsId=66666UF6EVsSyXTtMXfamxz6EVtQEVs6EVs6EVs6E666666--&fn=app_realitytesting299.pdf

[10] Forrest, E., 2009, "Nanoscale Modification of Key Surface Parameters to Augment Pool Boiling Heat Transfer and Critical Heat Flux in Water and Dielectric Fluids" Master's thesis, MIT, Cambridge, MA.

[11] Remes, D., 2009, "Biosensor based on a MOS capacitor with an internal reference electrode" Master's thesis, Linköping University, Linköping, Sweden.